World Scientific
www.worldscientific.com

PRICING SOVEREIGN CONTINGENT CONVERTIBLE DEBT

ANDREA CONSIGLIO[*,‡], MICHELE TUMMINELLO[*,§] and
STAVROS A. ZENIOS[†,¶]

Department of Economics, Business & Statistics
University of Palermo, Viale delle Scienze
90145 Palermo, Italy

†*Department of Accounting & Finance, University of Cyprus*
P.O. Box 20537, CY-1678 Nicosia, Cyprus

Wharton Financial Institutions Center, University of Pennsylvania, USA

Non-Resident Fellow, Bruegel, Belgium
‡*andrea.consiglio@unipa.it*
§*michele.tumminello@unipa.it*
¶*zenios.stavros@ucy.ac.cy*

We develop a pricing model for Sovereign Contingent Convertible bonds (S-CoCo) with payment standstills triggered by a sovereign's Credit Default Swap (CDS) spread. We model CDS spread regime switching, which is prevalent during crises, as a hidden Markov process, coupled with a mean-reverting stochastic process of spread levels under fixed regimes, in order to obtain S-CoCo prices through simulation. The paper uses the pricing model in a Longstaff–Schwartz American option pricing framework to compute future state contingent S-CoCo prices for risk management. Dual trigger pricing is also discussed using the idiosyncratic CDS spread for the sovereign debt together with a broad market index. Numerical results are reported using S-CoCo designs for Greece, Italy and Germany with both the pricing and contingent pricing models.

Keywords: Contingent bonds; sovereign debt; debt restructuring; regime switching; credit default swaps.

1. Introduction

The Eurozone crisis and the record-breaking Greek sovereign default in particular (technically, a restructuring), highlighted the need for international legal procedures to deal with sovereign defaults. In September 2015 the United Nations General Assembly adopted a resolution on "Basic Principles on Sovereign Debt Restructuring Processes".[a] With the debate on appropriate legal mechanisms ongoing, see,

---

[a]Resolution A/69/L.84 at http://unctad.org/en/pages/newsdetails.aspx?OriginalVersionID=1074.

e.g. Li (2016), proposals have also emerged for financial innovation solutions to the problem. Sovereign contingent convertible bonds (S-CoCo) with automatic debt payment rescheduling, have been suggested in academic and policy papers as a potential solution to sovereign debt crises (Consiglio & Zenios 2015, Brooke *et al.* 2013, Barkbu *et al.* 2012). These papers advance several arguments on the merits of contingent debt for sovereigns which we do not repeat here. Our contribution was to make these proposals concrete by suggesting a payment standstill mechanism triggered when the sovereign's CDS spread exceeds a threshold, and to develop a risk optimization model demonstrating how contingent debt improves a country's debt risk profile. An alternative proposal are GDP-linked bonds with coupon payments linked to a country's GDP level or GDP growth, see, e.g. Kamstra & Shiller (2009), Borensztein & Mauro (2004), Bank of England (2015), Consiglio & Zenios (2018). These instruments are quite distinct from S-CoCo, and the pros and cons of each are discussed in Bank of England (2015), highlighting the quest for financial innovation solutions to sovereign debt crises.

The IMF recently published a staff report with an extensive technical annex IMF (2017a, 2017b) discussing broadly defined sovereign contingent debt instruments (SCDI) as a "countercyclical and risk-sharing tool", which "remain[s] appealing". One of the three specific types of instruments are "*extendibles*, which push out the maturity of a bond if a pre-defined trigger is breached".

Our contributions are, first, to develop a pricing model for one type of extendibles, and, second, to develop state contingent pricing of these instruments for risk management. To achieve these objectives, we model a mean-reverting stochastic process of CDS spreads. However, the risk factors underlying spread changes are time-dependent and shocks are persistent, and the risk models could break down during a crisis when they are most needed. To address this salient issue we develop models under regime switching, and this is a significant innovation of the paper.

We hasten to add that our contribution does not settle the debate on market-based versus institutional-based triggers, or the debate on extendibles versus GDP-linked bonds. However, it contributes to an understanding of the pricing of sovereign contingent debt, its risk profile, and how design parameters can affect prices and risks.

Justification for using CDS spreads as the trigger is found in existing literature. An appropriate trigger must be accurate, timely and defined so that it can be implemented in a predictable way (Calomiris & Herring 2013). CDS spreads qualify. More importantly, the trigger should be comprehensive in its valuation of the issuing entity, and current literature shows that the CDS market is becoming the main forum for credit risk price discovery.

Having established CDS spreads as appropriate early indicators for credit risk, the question is then raised on how to model their dynamics. Investigations on what drives CDS spreads identify global changes in investor risk aversion, the reference country's macroeconomic fundamentals, and liquidity conditions in the

CDS market (Badaoui *et al.* 2013, Fabozzi *et al.* 2016, Longstaff *et al.* 2011), but the relative importance of such factors changes over time (Heinz & Sun 2014). Amato & Remolona (2003) observe that yield spreads of corporate bonds tend to be many times wider than what would be implied by expected default losses alone — a "credit spread puzzle" — so that research has been focusing on modeling CDS spread returns directly, instead of modeling their response to market fundamentals. This approach is advocated by Cont & Kan (2011) who provide modeling guidance by analyzing stylized facts of corporate CDS spreads and spread returns. Their work identified important properties of the dynamics of CDS spread returns — stationarity, positive auto-correlations, and two-sided heavy tailed distributions — and they proposed a heavy-tailed multivariate time series model to reproduce the stylized properties. Brigo & Alfonsi (2005) develop a shifted square-root diffusion model for interest rate and credit derivatives, and O'Donoghue *et al.* (2014) develop a one-factor tractable stochastic model of spread-returns with mean-reversion (SRMR) as an extension of Orstein–Uhlenbeck process with jumps.

These models were developed for corporate CDS but in principle they could be used for sovereign CDS as well. However, there is a prevalent issue with *regime switching* in the sovereign market, especially during crises. This became apparent to us while calibrating the SRMR model to Greek sovereign CDS spread data for our earlier paper. Calibration was unsuccessful for the period December 2007–February 2012, but converged when applied to different regimes identified using the test of Bai & Perron (1998). Therefore, we develop the regime switching mechanism instead of the jump process, and maintain the mean-reversion one-factor model of spread returns within each regime.

Regime switching in CDS spreads has been studied systematically by others as an empirical feature of the market, but, to the best of our knowledge, did not receive any attention in CDS pricing literature. Fontana & Scheider (2010) find that euro area credit markets witnessed significant repricing of credit risk in several phases since 2007. They find a structural break in market pricing, which coincides with the sharp increase in trading of CDS and declining risk appetite of investors since summer 2007, and attribute these changes to flight-to-liquidity, flight-to-safety, and limits to arbitrage. Regime switching in the corporate CDS market was identified by Cont & Kan (2011) who find the behavior of spreads "clearly divided into two regimes: before and after the onset of the subprime crisis in 2007". These observations are consistent with the analysis of Augustin (2014) who finds that CDS spreads change abruptly in response to major financial events, such as, for instance, the Bear Stearns bailout and Lehman Brothers bankruptcy, and are very persistent otherwise, over a sample of 38 countries in the period from 9 May 2003 to 19 August 2010. Alexander & Kaeck (2008) examine the empirical influence of a broad set of determinants of CDS spreads listed in iTraxx Europe, and find that, while most theoretical variables do contribute to the explanation of spread changes, their

influence depends on market conditions. CDS spreads may behave differently during volatile periods compared to their behavior in tranquil periods. Using a Markov switching model they find evidence supporting the hypothesis that determinants of credit spreads are regime specific. Castellano & Scaccia (2014) find that, for corporate CDS, it is the volatility of returns that carries the signal, and they model regime switching using a hidden Markov matrix. Not only there is ample empirical evidence of regime switching, there are also theoretical arguments to support the observations. Arghyrou & Kontonikas (2016) use earlier models by Krugman and Obstfeld to argue that Greece can be in one of three regimes: one with credible commitment to stay in the eurozone with guarantees of fiscal liabilities, one that guarantees fiscal liabilities for as long the country stays in the eurozone but uncertainty about the country's commitment to do so, and one without fully credible commitment to the eurozone.

Regime switching is a salient feature for our work because of the payment standstill triggered in case of a crisis, and crises typically signal a regime switch. For instance, during the eurozone crisis, a sharp drop of CDS spreads was noted across the board in the second half of 2012 following the ECB OMT announcement, and this was primarily due to a switch of the investors' sentiment, while country specific fundamentals remained broadly unchanged (Heinz & Sun 2014). Hence, we develop our model with regime switching.

The rest of the paper develops the pricing model, and uses it to develop state-dependent prices at some risk horizon and simulate holding period returns. We start in Sec. 2 with a statistical analysis of CDS spreads and spread returns for sovereigns in the eurozone periphery and core countries, and identify regime switching. This section informs our modeling work by giving a descriptive analysis of the eurozone sovereign CDS market. Section 3 develops the scenario generating stochastic processes for both regime switching and steady state for CDS spreads, spread returns and risk free rates. Section 4 develops the pricing model, state-contingent pricing, and holding period return scenarios. We illustrate numerically for a eurozone crisis country (Greece) and core countries (Germany and Italy). Section 5 concludes. The asymptotic modeling of CDS spreads — as opposed to spread returns addressed in existing literature — is given in Appendix A.

2. Some Observations on Sovereign CDS Spreads

A pricing model should be guided by the stylized facts of the observed series. The simulation window for pricing S-CoCo is twenty to thirty years, and the risk horizon for state contingent S-CoCo pricing is ten to twenty years, so we focus on long term characteristics of the data generating process. We model and calibrate the limiting dynamics of spreads (Appendix A), so we need the statistics describing time-dependent equilibria of the process. These equilibria are the *regimes*.

In Consiglio *et al.* (2017) we analyzed the five-year CDS spread for a sample of European countries using daily data from February 2007 to March 2016. The test

of Bai & Perron (1998) applied to the spread level identifies regime changes for all countries in the sample.[b] Some countries, such as France, Italy, Portugal, Spain, and Cyprus, are synchronized in their regime switching, whereas Germany, Ireland, and Greece have idiosyncratic regime changes. For instance, only Germany had a regime switch associate with the subprime crisis and the collapse of Lehman Brothers in September 2008, while the onset of the eurozone crisis in spring 2010 signals regime switching for all countries. Ireland and Greece had their own idiosyncratic banking and sovereign debt crises, respectively, which ushered in new regimes. Figure 1 illustrates the CDS spreads and identifies regime changes for the three countries we will be using to test our pricing models. In particular, Germany with very low spread levels and low volatility, Greece with excessive debt undergoing a major crisis, and Italy with high debt levels and medium CDS spreads. Figure 2 displays the five-year CDS spreads for Greece, highlighting the major events that impact spreads, as summarized in Table 1. April 2010 signals switching from a *tranquil* to a *turbulent* regime of the Greek economy, and the events clustered around the change of regime are given in the table. The change of regime in July 2011 is the run up to the Greek PSI signaling the start of the Greek debt crisis. The events highlighted involve an open letter to European and international authorities by German finance minister Schäuble about "fair burden sharing between taxpayers
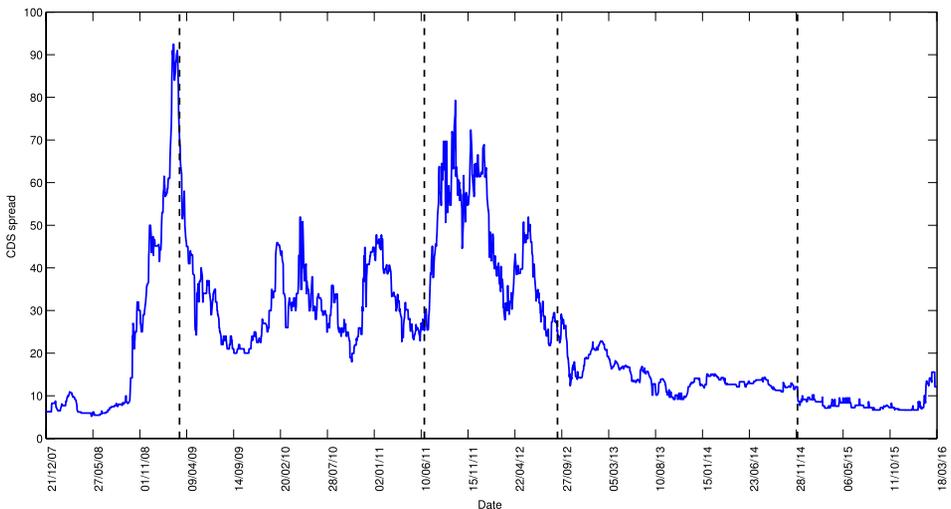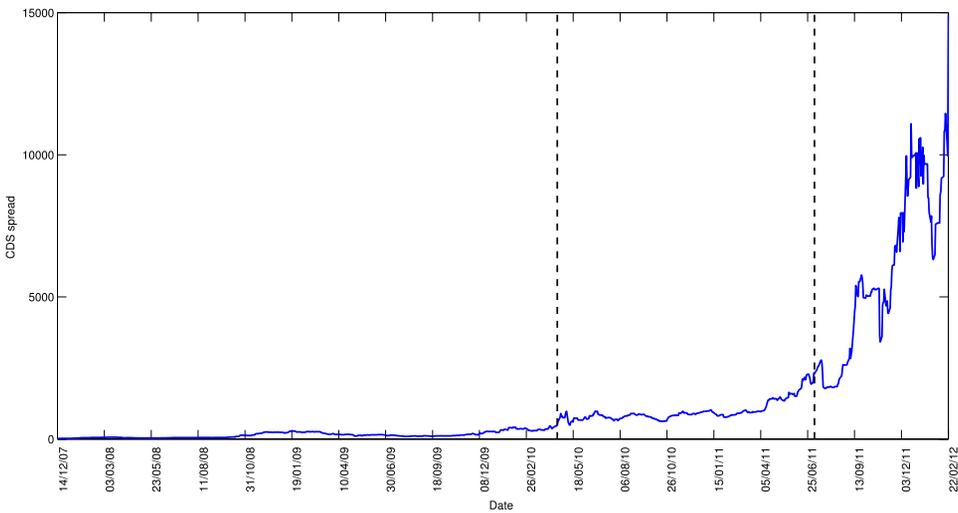

(a) Germany

Fig. 1. Regime switching identified using Bai and Perron test for the countries used to test the pricing models. Regimes are different for each country analyzed. Specifically, they differs in turmoil periods, whereas calm periods are basically the same.

[b]We use the Bai-Perron test in the free software system R.
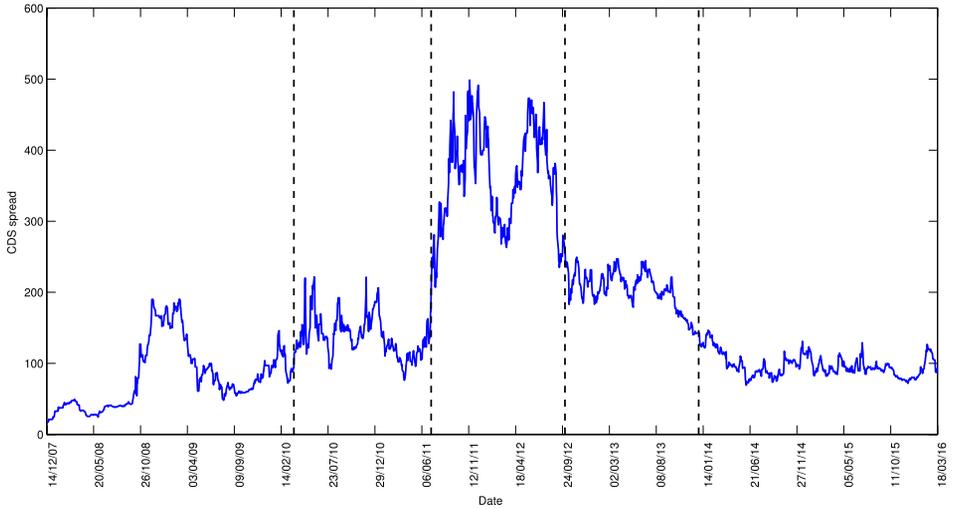
(b) Italy

(c) Greece

Fig. 1. (*Continued*)

and private investors" in providing financial support to Greece, and Jean-Claude Juncker's backing Germany's proposal arguing for "soft debt restructuring" with private sector participation.

The mean and standard deviation of CDS spreads and spread returns for different regimes are in Table 2 for Germany, Greece, and Italy. These quantities are needed to calibrate the simulation model. We focus on regime switching for the spreads, but regime breaks can also be identified for the volatilities as suggested by
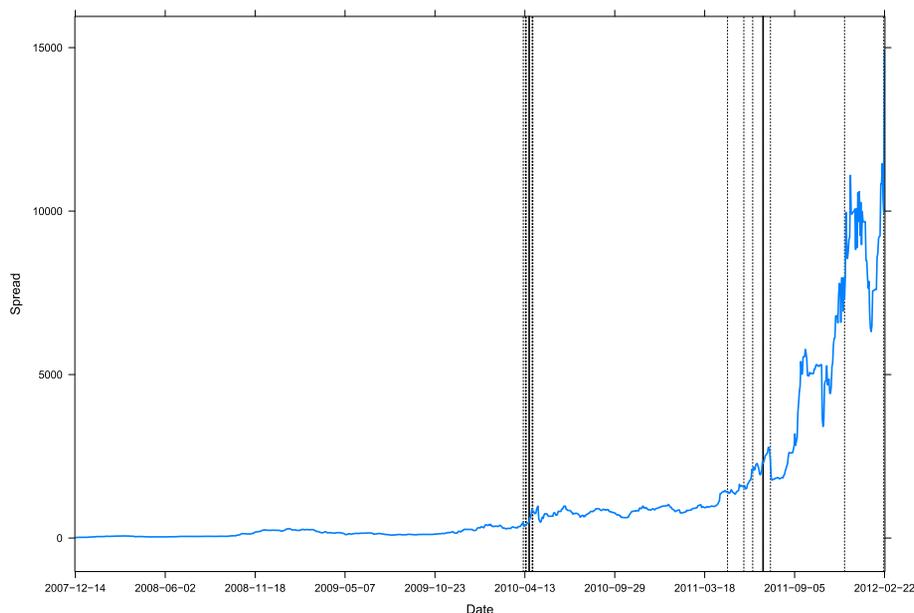
Fig. 2. Time series of the five-year CDS for Greece. Vertical dotted lines denote events which affect CDS spreads as given in Table 1. These events usher in new regimes that can be identified using Bai–Perron test and denoted by the vertical solid lines.

Castellano & Scaccia (2014). A comprehensive empirical analysis of the sovereign CDS markets, its statistical properties, and regime switching analysis including regime switching identification with common regimes, is reported in Consiglio *et al.* (2017).

Table 1. Major events relating to the Greek sovereign crisis regime switch of July 2011.

25 Feb 10	EU and IMF mission in Athens delivers grim assessment of country's finances
16 Mar 10	Eurozone finance ministers agree to help Greece but reveal no details
19 Mar 10	Prime Minister Papandreou warns Greece may have to go to the IMF
22 Mar 10	President Barroso urges member states to agree aid package for Greece
12 Apr 10	Greece announces that first trimester deficit was reduced by 39.2%
13 Apr 10	EU leaders agree bailout plan for Greece
14 Apr 10	ECB voices its support for the rescue plan of Greece

Table 2. CDS spread and spread return statistics in each one of the regimes identified using Bai–Perron test.

Country	Regime	Spread mean	Spread std. dev.	Spread return std. dev.
Germany	21 Dec 07–13 Mar 09	22.22	23.54	5.48
	16 Mar 09–20 Jun 11	31.69	8.85	5.48
	21 Jun 11–12 Sep 12	45.60	13.98	6.24
	13 Sep 12–02 Dec 14	14.64	3.73	3.95
	03 Dec 14–18 Mar 16	8.25	1.93	6.31

Table 2. (*Continued*)

Country	Regime	Spread mean	Spread std. dev.	Spread return std. dev.
Greece	14 Dec 07–20 Apr 10	146.09	103.90	4.45
	21 Apr 10–06 Jul 11	980.27	363.36	5.20
	07 Jul 11–22 Feb 12	5770.43	2917.45	8.05
Italy	14 Dec 07–29 Mar 10	79.71	45.48	5.01
	30 Mar 10–07 Jul 11	137.69	28.54	6.51
	08 Jul 11–02 Oct 12	361.94	68.99	4.94
	03 Oct 12–27 Dec 13	203.73	26.66	2.91
	30 Dec 13–18 Mar 16	97.31	15.82	3.67

3. Scenario Generating Process

Our scenario generator consists of a core process which determines regimes of the expected value of the CDS spread, and a process of the dynamics of the CDS spread superimposed on the mean value in each regime. In the next two subsections we model these sub-processes.

3.1. *Regime switching process*

We assume that regime transitions are driven by a discrete time-homogeneous Markov chain with finite state space $\mathcal{R} = \{1, 2, \ldots, S\}$, where

$$p_{ij} = \mathbb{P}(X_k = j \,|\, X_{k-1} = i)$$

is the transition probability of switching from regime i at time $k - 1$ to regime j at time k. The transition probabilities matrix $P = \{p_{ij}\}$ is a stochastic matrix, i.e. $p_{ij} \geq 0$, for all $i, j \in \mathcal{R}$, and $\sum_{j \in R} p_{ij} = 1$, for all $i \in \mathcal{R}$.

The transition matrix P is fundamental to simulating a regime switching process. However, it cannot be estimated from observed historical series because regime breaks are rare events. Instead we infer P from an estimate of the limiting probability π^* (see definition below). We denote by $\pi_i^{(k)}$, for all $i \in \mathcal{R}$, the distribution at time k of a Markov chain X,

$$\pi_i^{(k)} = \mathbb{P}(X_k = i). \tag{3.1}$$

Given a transition matrix P, it is possible to show that

$$\pi_j^{(k)} = \mathbb{P}(X_k = j) = \sum_{i \in \mathcal{R}} \mathbb{P}(X_k = j \,|\, X_{k-1} = i)\mathbb{P}(X_{k-1} = i) = \sum_{i \in \mathcal{R}} p_{ij} \pi_i^{(k-1)}. \tag{3.2}$$

If we denote by $\pi^{(k)}$ the row vector of probabilities $(\pi_1^{(k)}, \ldots, \pi_S^{(k)})$, then (3.2) is written in matrix form as

$$\pi^{(k)} = \pi^{(k-1)} P. \tag{3.3}$$

Row vector of probabilities π^* is a *stationary distribution* for the Markov chain X_k, $k > 0$, if

$$\pi^* = \pi^* P, \quad \text{i.e. } \pi_j^* = \sum_{i \in \mathcal{R}} \pi_i^* p_{ij}. \tag{3.4}$$

Note that π^* does not necessarily exist, nor it is unique. If π^* exists and is unique then we can interpret π_i^* as the average proportion of time spent by the chain X in state i.

Given P, the stationary probability distribution π^* is obtained as the solution, if it exists, of the following system:

$$\pi^* = \pi^* P, \tag{3.5}$$

$$\pi^* \mathbf{1} = 1, \tag{3.6}$$

$$\pi^* \geq 0. \tag{3.7}$$

We assume that the stationary distribution can be estimated by the average number of days the CDS spread process is in regime i,

$$\hat{\pi}_i^* = \frac{\text{Number of days CDS spread is in regime } i}{\text{Number of total days in sample}}. \tag{3.8}$$

This is a reasonable assumption for long horizons, but any estimate of the probability of a country being in a given regime can be used as well. For instance, we can use the transition probabilities of the rating agencies to estimate the likelihood of a country migrating to a better or worse regime from where it is at present. Each rating class implies a probability of sovereign default and, consequently, a CDS regime, so that the migration probabilities provide an estimate of the stationary distribution. In Sec. 4.1 we carry out sensitivity analysis on the impact of these estimates on S-CoCo prices.

A constraint set on P is obtained by the properties of square matrices from linear algebra theory. In particular, let us assume that the Markov matrix $P = (p_{ij}) \in \mathbb{R}^{S \times S}$ has S distinct eigenvalues denoted by $\lambda = [\lambda_1 \lambda_2 \ldots \lambda_S]$.[c] Since P is a stochastic matrix, the eigenvalue with highest magnitude has absolute value equal to one, $|\lambda_1| = 1$, and according to the Perron–Frobenius theorem $1 = \lambda_1 > |\lambda_i|$, for all $i = 2, 3, \ldots, S$. Denote by ξ_i the row vector which is the left eigenvector associated with the eigenvalue λ_i of P, and denote by ν_i the column vector which is the right eigenvector of the same λ_i, with ξ_i and ν_i obtained by solving

$$\xi_i P = \lambda_i \xi_i, \tag{3.9}$$

$$P \nu_i = \lambda_i \nu_i. \tag{3.10}$$

---

[c]We are using matrix diagonalization, and the same conclusions are obtained when eigenvalues are not distinct, but the corresponding eigenvectors are linearly independent. Since we can arbitrarily choose to have a transition matrix with distinct eigenvalues, we present our analysis only for this case.

Note that the left and right eigenvectors are orthonormal, so $\xi_i \cdot \nu_j = \delta_{ij}$, where δ_{ij} is the Kronecker delta.

Also observe that the right eigenvector for $\lambda_1 = 1$ is a unit vector as P is a stochastic matrix and all the rows sum up to 1, i.e.

$$P\nu_1 = \nu_1. \tag{3.11}$$

Furthermore, if P is the transition matrix of a stationary process, then the left eigenvector for λ_1 is the steady distribution $\xi_1 = \pi^*$, and we have

$$\xi_1 P = \xi_1. \tag{3.12}$$

Denote by $U = (u_{ij})$ a matrix whose columns are the right eigenvectors of P, and by $V = (v_{ij})$ a matrix whose rows are the left eigenvectors of P. Then P can be written as

$$P = UDV, \tag{3.13}$$

where $D = (d_{ij})$ is a diagonal matrix whose entries are the eigenvalues of the transition matrix P, $D = \lambda I_S$. Recall that the eigenvectors are orthogonal so that $UV = I_S$. Moreover, the first column of V has all entries equal to 1, and if P admits a steady state, the first row of U is the stationary distribution. If P is diagonalizable, it can be proved that the kth power of P can be written as

$$P^k = \sum_i \lambda_i^k \xi_i \nu_i. \tag{3.14}$$

Since $\lambda_1 = 1$, and $|\lambda_i| < 1$, for $i = 2, 3, \ldots, S$,

$$\lim_{k \to \infty} P^k = \xi_1 \nu_1, \tag{3.15}$$

where it can be proved that the speed of convergence is given by the magnitude of λ_2, and P converges faster to the steady state π^* for smaller values of $|\lambda_2|$.

Essentially, we model P to deliver the limiting distribution $\hat{\pi}_i^*$. This is an inverse problem and, in general, there are infinitely many Markov matrices P that give a steady state distribution $\hat{\pi}_i^*$. To single out a distribution, we use the maximum entropy principle, which postulates that given partial information about a random variable we should choose that probability distribution for it, which is consistent with the given information, but has otherwise maximum uncertainty associated with it (Kapur 1989). The resulting estimates are the least biased or maximally uncommitted with respect to missing information. The maximum entropy principle is derived from information theory, originating in the work of Shannon (1948) and has been justified in numerous applications, such as matrix estimation including the estimation of transition probability matrices (Schneider & Zenios 1990). For applications to image reconstruction, economics, and other areas see (Censor & Zenios 1997, Chap. 9). We therefore, estimate the Markov matrix P that satisfies

the above properties while maximizing Shannon's entropy, by solving:

$$\text{Maximize}_{p_{ij}} \quad -\sum_{ij} p_{ij} \log p_{ij}, \tag{3.16}$$

$$\text{s.t.} \quad \sum_{k} u_{ik} v_{kj} = \delta_{ij}, \quad \text{for all } i, j \in \mathcal{R}, \tag{3.17}$$

$$\sum_{k} u_{ik} d_{kk} v_{kj} = p_{ij}, \quad \text{for all } i, j \in \mathcal{R}, \tag{3.18}$$

$$\sum_{j} p_{ij} = 1, \quad \text{for all } i \in \mathcal{R}, \tag{3.19}$$

$$p_{ij} \geq 0, \quad \text{for all } i, j \in \mathcal{R}, \tag{3.20}$$

where $u_{i1} = 1$, for all $i \in \mathcal{R}$, is the constraint defining the right eigenvector associated with λ_1. Constraints $v_{1j} = \hat{\pi}_j^*$, for all $j \in \mathcal{R}$, ensure that the left eigenvector associated with λ_1 is equal to the empirically estimated steady-state distribution. Eq. (3.16) is obtained from the additivity property of Shannon's entropy, i.e. the conditional entropy $H(X_k \,|\, X_{k-1})$ is calculated as

$$H(X_k \,|\, X_{k-1}) = \sum_{i} H(X_k \,|\, X_{k-1} = i)$$

$$= \sum_{i} \left[-\sum_{j} p_{ij} \log p_{ij} \right]$$

$$= -\sum_{ij} p_{ij} \log p_{ij}. \tag{3.21}$$

This is a small scale quadratically constrained nonlinear optimization problem. The number of variables is equal to the number of regimes squared, i.e. 25 for Germany and Italy, and 9 for Greece as identified by the Bai–Perron tests (Table 2). It can be solved using off the shelf packages, such as CONOPT (Drud 2005) used in our numerical results.

The eigenvalues of P are set to some arbitrary values, recalling that $d_{11} = \lambda_1 = 1$ and $d_{11} > d_{22} > \cdots > d_{SS}$. The possibility to arbitrarily set the eigenvalues of P allows control on the expected number of time steps that the process spends consecutively in the same state. The trace of a matrix is invariant under rotation, which implies

$$S \geq \sum_{i=1}^{S} \lambda_i = \sum_{i=1}^{S} p_{ii}. \tag{3.22}$$

The expected number of consecutive time steps, $E(D_i)$, that the process spends on state i is

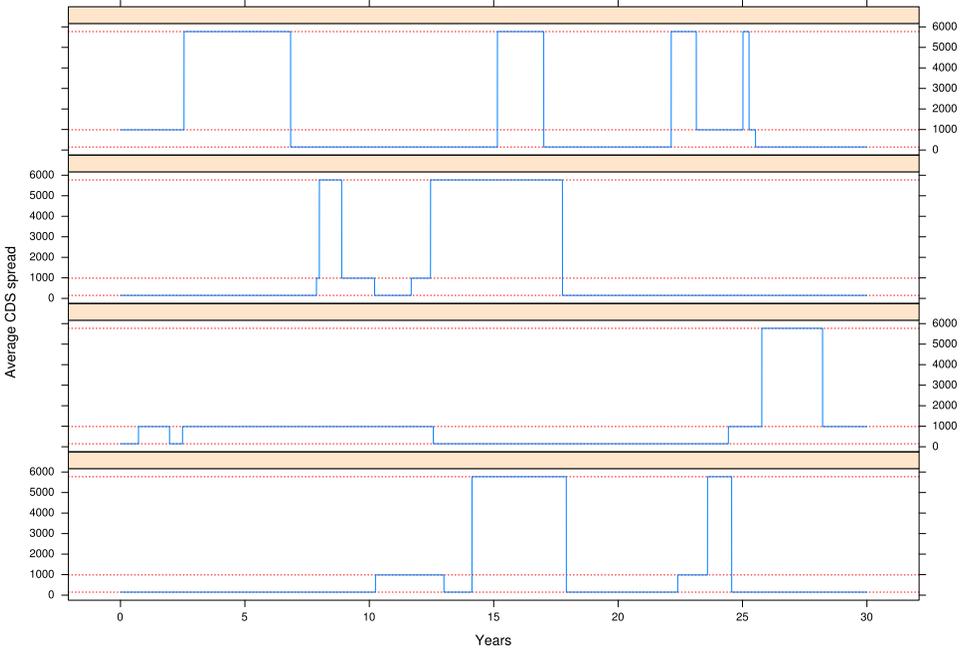$$E(D_i) = \sum_{k=1}^{\infty} k p_{ii}^{k-1} (1 - p_{ii}) = \frac{1}{1 - p_{ii}}. \tag{3.23}$$

Fig. 3. Simulation of regimes on a daily basis over a thirty-year horizon for Greece. Solid lines illustrate the Markov process switching regimes, and a regime is defined by the average spread (dotted lines) estimated from historical data for each regime.

Equation (3.22) indicates that the average of eigenvalues is equal to the average value of p_{ii} over the allowed states. Therefore, if one sets eigenvalues $\lambda_2, \lambda_3, \ldots, \lambda_S$ close to 1, then also the average value of p_{ii} turns out to be close to 1, and, according to Eq. (3.23), the expected number of time steps that the process consecutively spends on a given state is large on average. On the contrary, if eigenvalues $\lambda_2, \lambda_3, \ldots, \lambda_S$ are small, then probabilities p_{ii} are also small.

Figure 3 displays four regime scenarios for Greece, generated by simulating a Markov chain with daily frequency over a thirty-year horizon. We generate scenarios based on the means spread value of the three regimes from Table 2, set monotonically decreasing eigenvalues close to 1 to obtain reasonable persistence in each regime, and obtain the empirical steady-state distribution using (3.8). Solving (3.16)–(3.20) we obtain the following transition matrix for Greece's regimes:

$$P = \begin{pmatrix} 0.9982 & 9.62\text{E}{-}4 & 7.89\text{E}{-}4 \\ 8.03\text{E}{-}4 & 0.9985 & 6.56\text{E}{-}4 \\ 2.62\text{E}{-}4 & 2.76\text{E}{-}4 & 0.9995 \end{pmatrix}. \tag{3.24}$$

We also calibrate the model for a country with less volatile spreads (Italy) and for a stable environment (Germany) and observe similar results (see Fig. 4). Note
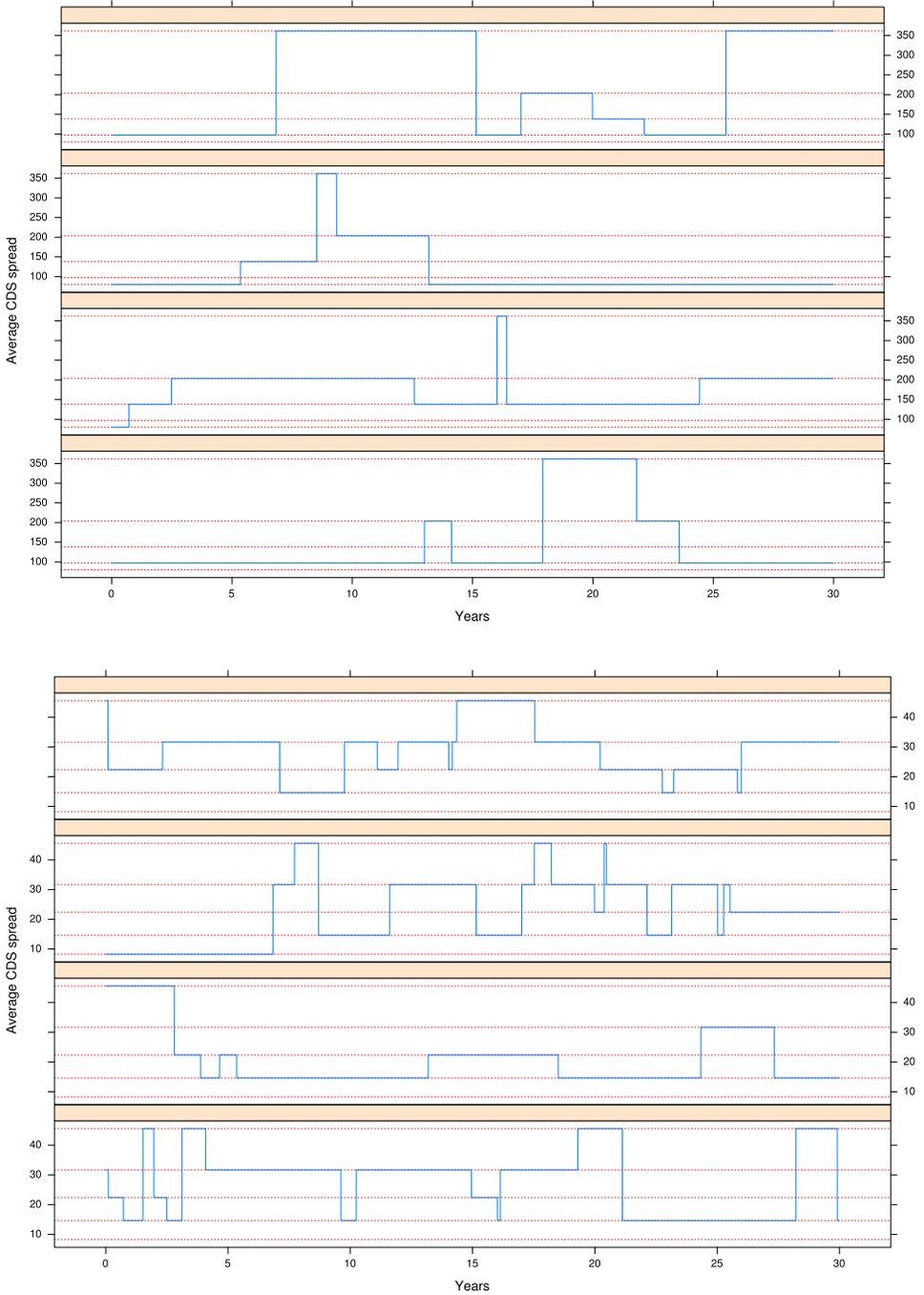
Fig. 4. Simulation of regimes on a daily basis over a thirty-year horizon for Italy (top) and Germany (bottom). Solid lines illustrate the Markov process switching regimes, and a regime is defined by the average spread (dotted lines) estimated from historical data for each regime.

that for Germany the mean levels of the empirically observed regimes are close to each other and modeling regime switching is not necessary. (Of course, a user may specify extreme scenarios for a German spread crisis.)

3.2. *CDS and interest rate process*

We now superimpose the CDS spread process on the spread mean regimes generated by the Markov process. Broadly speaking, we generate scenarios of CDS spreads around the regime dynamics. We need a mean-reverting process that reverts to the mean CDS spread of the (simulated) regime. Furthermore, the variance should be bounded and the spread should be nonnegative. The SRMR model of O'Donoghue *et al.* (2014) for CDS spread returns belongs to the class of Ornstein–Uhlenbeck processes and has the nice property that the variance of the log-returns is bounded with time, thus providing a process that does not deviate excessively from its expected value for long intervals and remains nonnegative. In Appendix A, we derive the conditions on the parameters of this model so that asymptotically it converges to the regime mean values. Thus, we calibrate a stochastic process that has the desirable empirically observed properties of CDS spreads and spread returns, and conforms to the regime switches. With this approach the process dynamics capture not only the long-term mean spread but also spread and spread return volatility in each regime. Furthermore, as explained in Appendix A, this process allows to calibrate short term fluctuations and hence the smoothness of the curve.

Figure 5 illustrates a sample scenario of Greek CDS spread, around the regime scenario from Fig. 3 (top panel). The simulation is run on a daily basis over a thirty-year horizon. The process follows the mean CDS spread level for each regime. A first impression is of a process with unrealistic jumps of the spread coinciding with regime switching. Moreover, the dynamics of the spread for the tranquil regime appear to be flat, with negligible volatility. This is due to *y*-axis scaling to capture the wide range of spreads for Greece over a long horizon. Zooming in at the simulated series we observe a smooth transition between regimes, with higher volatility even in the tranquil regime. Figure 6 displays the spread dynamics between years twenty-five and twenty-six, where there are three consecutive regime transitions. Transition from crisis to turbulent regime is abrupt, but the spread changes with a reasonable gradient, as seen in the inset of the figure.

One desirable property of the model is the bounded variance of the stochastic process. Figure 5 (bottom) illustrates the 5% and 95% quantiles of the CDS spreads obtained over 1000 simulations. We observe that volatility does not increase with time and is dependent only on the given regime, so that turbulent regimes have higher volatilities than tranquil regimes and crisis regimes even higher. The largest Greek CDS spread during the crisis was almost 15000, and was generated by our simulation at the 95% quantile.

As explained in the next session, the S-CoCo cashflows are discounted using the EURO AAA-rated bond yields (E-AAA for short). We simulate the E-AAA short
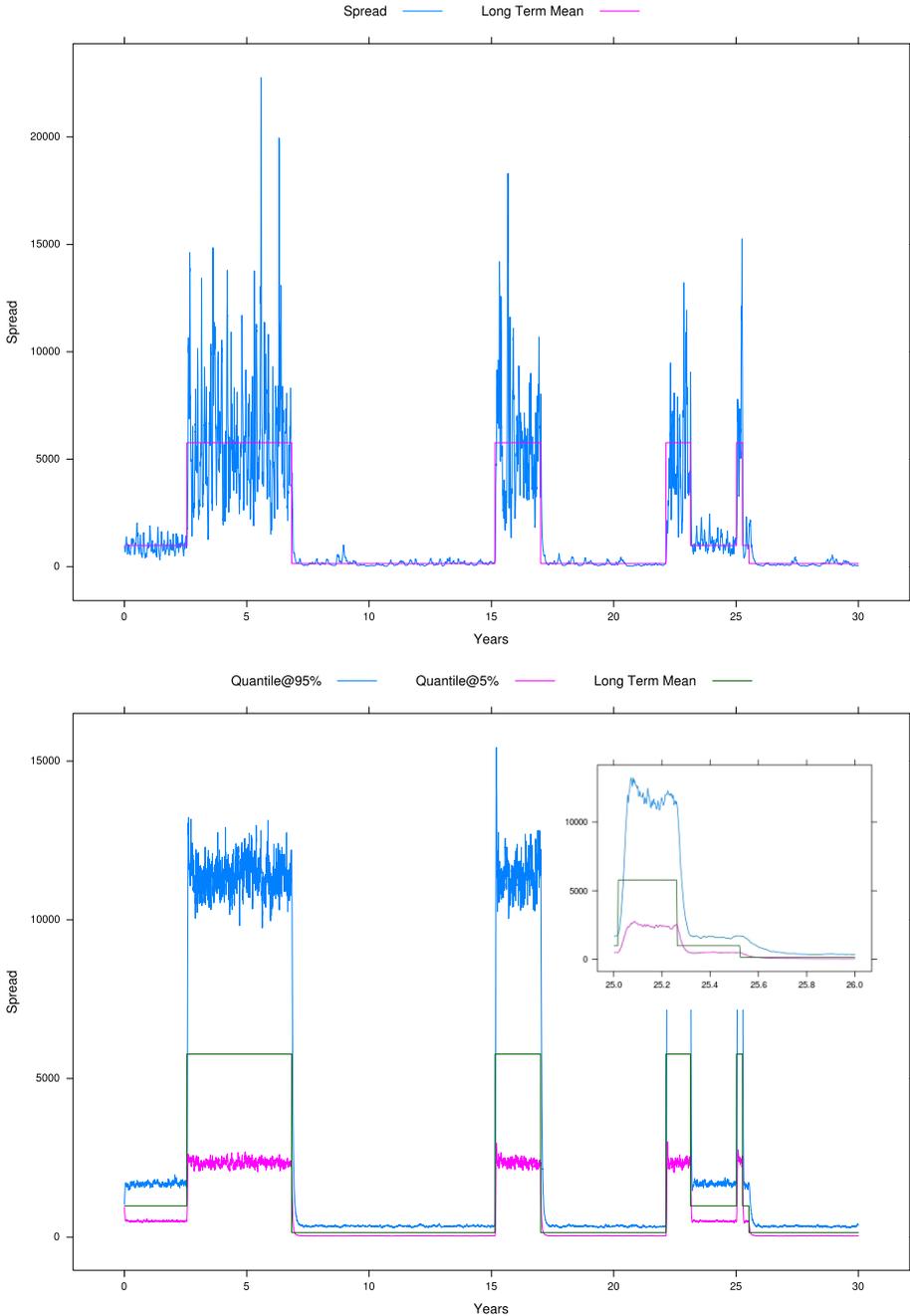
Fig. 5. A typical simulation path of the daily CDS spread for Greece over a thirty-year horizon (top) and the 5 and 95% quantiles over 1000 scenarios (bottom) with a detail of the spread dynamics between years twenty-five and twenty-six. The average spread of each regime is as estimated in Table 2.
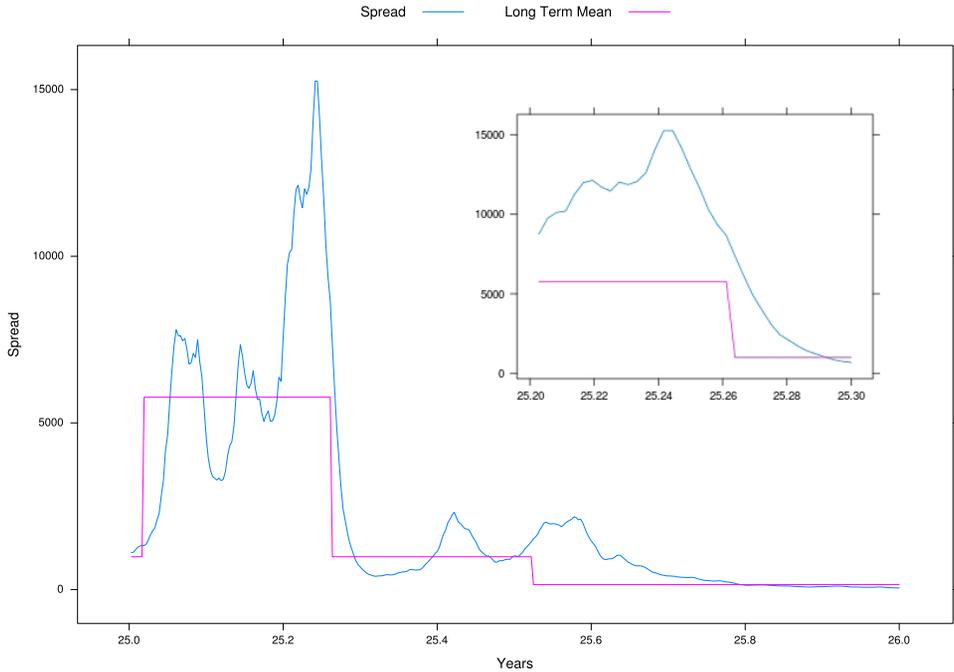
Fig. 6. Simulated daily CDS spread for Greece during regime switching from year twenty-five to year twenty-six. The CDS spread closely follows the average regime level and smoothly changes from one regime to another.

rate dynamics following the approach just described. To this purpose, we extract from the historical series of the E-AAA yield curve the series of the one-month rate, and we determine the regime sub-intervals and relative statistics to calibrate the model. We remark that this implementation does not match the term structure, and, therefore, we are not able to match observed bond prices on a given date. A workaround to this drawback would be to use a time-dependent process matching the actual forward curve, and calibrating the parameters of the model with given volatilities (implicit or historical ones). That is, unlike our implementation, where the process fluctuates around the simulated regimes, we could make the short rate to mean-revert towards an exogenously given forward curve.

4. Modeling Sovereign Contingent Convertible Debts

We develop now the pricing models using Monte Carlo simulations. Prices are obtained as the expected discounted cashflows from simulations of the Markov chain and the stochastic process of spreads and interest rates in each regime. We also show how to obtain state contingent prices at some risk horizon to facilitate risk management.

4.1. *Pricing*

We denote by $\xi = \{r_t, s_t\}$ the coupled stochastic process of the short rate r_t and CDS spread s_t, where we assume that $\mathrm{cov}[r_t, s_t] = 0$.[d]

To simplify notation, we use t to indicate discrete time steps, from the index set $\mathcal{T} = \{0, 1, 2, \ldots, T\}$. We draw from the probability distribution of ξ a discrete number of sample paths (*scenarios*), $\xi^l = \{r_t^l, s_t^l\}$, where $l \in \Omega = \{1, 2, \ldots, N\}$ and $t \in \mathcal{T}$. The time-discretized approximation of the stochastic process ξ, for each scenario $l \in \Omega$, is obtained from Eq. (A.1) by drawing N random samples of the diffusion term w_t from a Gaussian distribution. All sampled scenarios are equally likely with probability $1/N$, and large number of scenarios approximate the underlying Gaussian distribution. This is a standard Monte Carlo simulation, and converged well in our numerical implementation. For advanced variance reduction techniques see (Glasserman 2003, Chap. 4).

Denote by $\bar{s}$ the threshold of the CDS spread which activates the standstill. If at time t and under scenario l the CDS rate s_t^l hits $\bar{s}$, coupon payments are suspended for the next K periods. We define the set of time periods with payment standstill by $\mathcal{T}_m^l = \{t, t+1, \ldots, t+K\}$, and $m = 1, 2, \ldots, M$, where M is the number of times that the standstill mechanism is activated under scenario l, with the following properties:

(1) For any m and n, $\mathcal{T}_m^l \cap \mathcal{T}_n^l = \emptyset$, to preclude overlapping of payment standstills.
(2) For any $\tau \in \mathcal{T}_m^l$, $\tau > t$, if $s_\tau^l \geq \bar{s}$ the trigger signal is ignored, to avoid multiple triggering during a standstill interval.

The set of periods $t \in \mathcal{T}$ with payment standstill for scenario l is

$$\Lambda^l = \bigcup_{m=1}^{M} \mathcal{T}_m^l, \tag{4.1}$$

and we define an indicator function $\mathbb{1}_{\Lambda^l} : \mathcal{T} \to \{0, 1\}$ as

$$\mathbb{1}_{\Lambda^l}(t) = \begin{cases} 0, & \text{if } t \in \Lambda^l, \\ 1, & \text{if } t \notin \Lambda^l. \end{cases} \tag{4.2}$$

The standstill provision includes a special treatment of credit events occurring within K periods before maturity. In such cases, coupon payment standstill implies deferral of principal payment. In particular, denoting by $\mathcal{T}_Z^l$ the terminal standstill set under scenario l, and defining by J^l the first time step of $\mathcal{T}_Z^l$, $J^l = \min \mathcal{T}_Z^l$, the principal payment is delayed by $\Delta T^l = T - J^l + 1$, provided that $T - J^l < K$.

---

[d]We can also have correlated processes r_t and s_t. In this case, the covariance matrix will be factorized through a Cholesky decomposition, and standard Montecarlo sampling for correlated processes will be used to simulate jointly spread and interest rate, see Appendix A.

A. Consiglio, M. Tumminello & S. A. Zenios

The S-CoCo price is obtained as the expectation, over scenarios $l \in \Omega$, of the present value of coupon and principal payments. That is,

$$P_0 = \frac{1}{N} \sum_{l \in \Omega} \sum_{t \in \mathcal{T}} B^l(0,t) \mathbb{1}_{\Lambda^l}(t) c + B^l(0, T + \Delta T^l), \qquad (4.3)$$

where c is the coupon and $B^l(t,s)$ is the discount factor between time periods t and t'

$$B^l(t,t') = \exp \left\{ -\sum_{u=t}^{t'} r_u^l \right\}. \qquad (4.4)$$

There can be several variants of the standstill provision, such as payment standstill with an associated maturity extension for as long the spread exceeds the threshold. Also, there are various alternative ways to treat coupon payments missed during the standstill, such as resumption of nominal value payments until the (extended) maturity — this was our original S-CoCo suggestion — or resumption of payments on an accrual basis or total write-down of missed payments. The pricing formula still applies but modifications are needed of the definition of the triggering set Λ^l or a different accounting of cashflows in (4.3). Modifications are conceptually straightforward but complicate the notation and we do not give them here.

Using numerical line search we solve pricing formula (4.3) for c such that

$$P_0(c) = 1. \qquad (4.5)$$

The difference between c and the par rate of a AAA sovereign bond is the premium charged by investors to buy the S-CoCo.

Figure 7 displays par rates of a twenty-year S-CoCo for the three countries of our study with threshold $\bar{s} = 100, 200, 300, 400$. The CDS processes are calibrated on daily historical series from January 2007 to the end of 2016, except for Greece whose CDS trading was suspended at the end of 2012. The parameters of the short rate dynamics are inferred from the daily historical series of the E-AAA 1-month bond yield. Each par rate is computed by solving Eq. (4.5) over a set of 100 regime scenarios and 1000 interest rates and spread scenarios for each regime, for a total of 100000 paths of length twenty years and semi-annual time step. Also shown in the figure is the par rate of a plain AAA-rated bond (1.6%). Greece has the highest premium over the AAA-rated yield due to the very high average level of CDS spreads of the recent past. The premium increases as $\bar{s}$ is reduced since the probability of breaching the threshold increases with a commensurate increase in the number of standstill time periods. German S-CoCo is priced at par with AAA-rated bonds as the likelihood of German CDS spreads breaching even a very low threshold is virtually nil. The Italian spread is, naturally, between Greece and Germany.

Note that, the convergence of the par rate to the AAA level is due to the unique short rate dynamics used for all countries, which is calibrated on the AAA-rated bond historical yield series. Differentiation of the minimum par rate, and therefore,
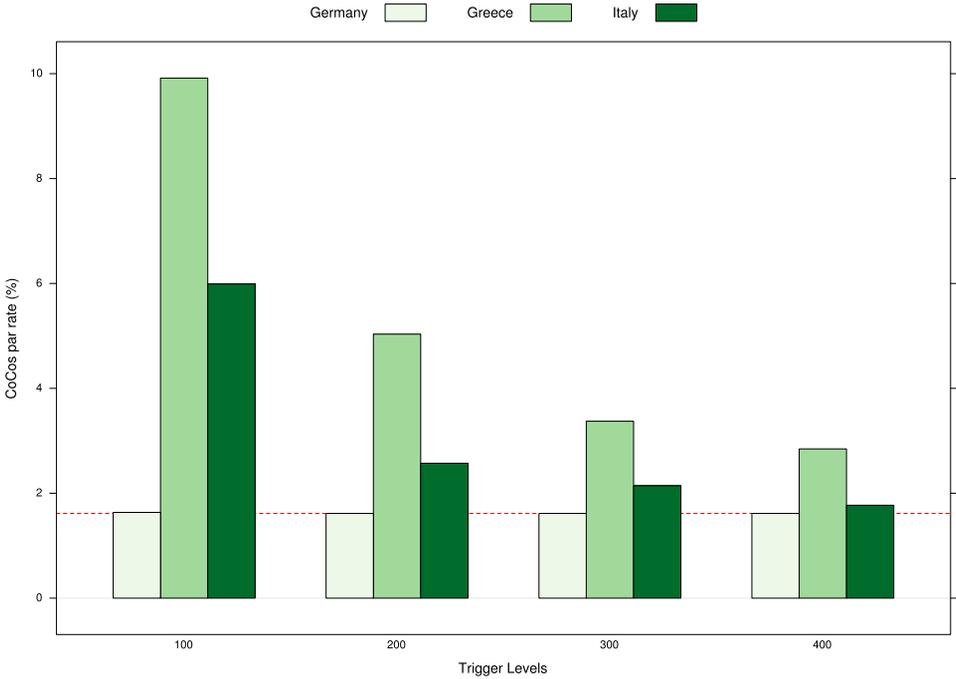
Fig. 7. Par rate of the S-CoCo versus trigger thresholds $\bar{s}$. The red dashed line indicates the par yield of a AAA-rated bond (1.6%). Greece and Germany are at the two opposite poles, whereas Italy is naturally between the two. This is a consequences of the very high average level of CDS spreads of the recent past for Greece and Italy. The very low likelihood that the German CDS spreads breaches any meaningful threshold makes its spread, with respect to plain bonds, virtually nil.

convergence to different minimum levels as $\bar{s}$ increases, would be observed if the short rate dynamics are calibrated separately for each country.

We illustrate the sensitivity of price and par rate estimates to changes of the regime probabilities. The experiment is for the Greek case where the Bai-Perron test identifies three regimes with estimated steady-state probability vector $\hat{\pi}^* = (0.5612, 0.2888, 0.15)$. We perturb $\hat{\pi}_i^*$ by sampling a Dirichlet distribution with parameters $\alpha\hat{\pi}^*$ (Kotz *et al.* 2005), where α is the *concentration parameter* determining how concentrated is the probability mass of a Dirichlet distribution around the given discrete probability distribution $\hat{\pi}^*$. The support of the Dirichlet distribution $\mathbb{D}(\alpha\pi)$ with $\pi \in [0,1]^N$, is the set of N-dimensional vectors $p = (p_1 p_2 \ldots p_N)$ whose entries are real numbers in the interval $(0,1)$, and the sum of the entries is 1. Equivalently, the domain of the Dirichlet distribution is itself a set of probability distributions, namely the set of N-dimensional discrete distributions.

In Fig. 8, we show the samples drawn from $\mathbb{D}(\alpha\hat{\pi}^*)$ where the concentration parameters are set to $\alpha = 10, 20, 30$. α can be viewed as the confidence of the decision maker about the estimate $\hat{\pi}^*$ of the steady state discrete distribution π^*,
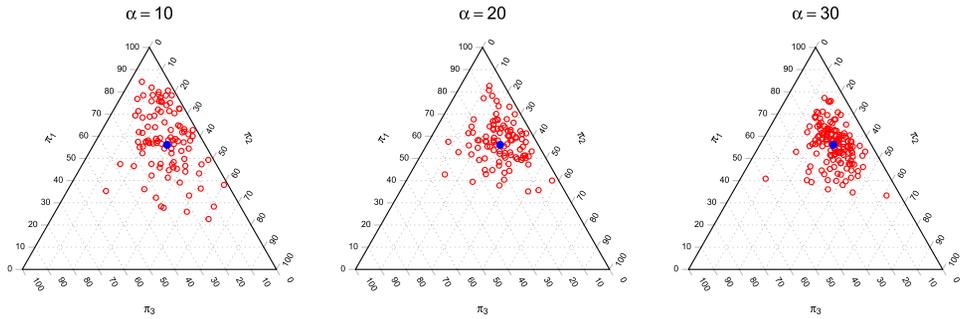
Fig. 8. Samples drawn (red circles) from a Dirichlet distribution $\mathbb{D}(\alpha\hat{\pi}^*)$ for different concentration parameters α. Higher values of α indicate more confidence about the estimate $\hat{\pi}^*$ (blue circle) and the samples are more concentrated around the estimate.

with higher α denoting more confidence that $\hat{\pi}^*$ is indeed a good estimate of the true π^*.

Given the sampled probability distributions p^l, with $l = 1, 2, \ldots, 100$, we estimate the price of a twenty-year S-CoCo with threshold 200. The distribution of prices is displayed using box-whisker plots, where the box delimits the inter-quartile range from 25% to 75% quantiles, whereas the black dot and the red star are, respectively, the median and the average price. The box-whisker plot of the CoCos price and par rates are displayed in Fig. 9. The inter-quartile range is quite stable for price estimate, ranging from 1.1% for high concentration value to 2.4% for low value. Higher sensitivity is displayed by par rates, with changes ranging from 60 bp for high concentration values to 126 bp for low concentration, due to the nonlinear relation between par rates and prices.

We remark here, that our pricing model does not guarantee that the price obtained is arbitrage-free. This is because we estimated the CDS spread and the
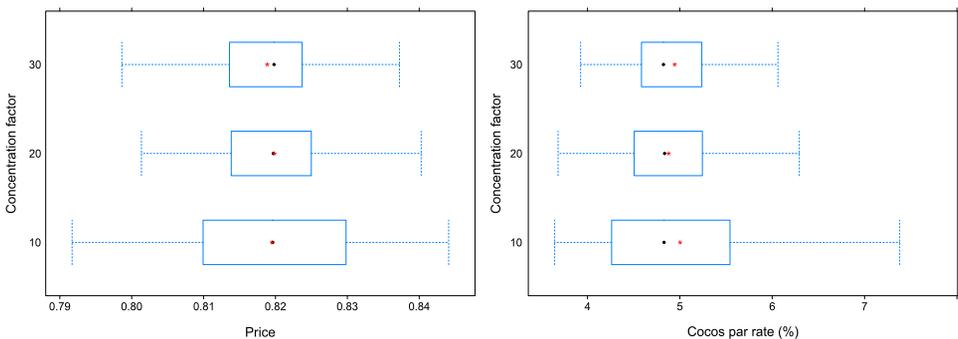

Fig. 9. Box-whisker plots of the prices (left panel) and par rates (right panel) for a twenty-year Greek S-CoCo with threshold 200. The perturbation of the estimated steady state distribution generates relatively stable prices but higher variability of par rates.

short rate dynamics under the objective measure $\mathbb{P}$. Our choice is motivated by the following arguments:

First, market-consistent pricing is typically obtained by fitting martingale models to quoted market prices, since any arbitrage opportunities would be quickly eliminated and priced out of a liquid market. S-CoCos bonds, however, do not exist yet and our analysis is to show that under certain circumstances sovereign welfare could benefit from introducing them.

Second, in general, for assets (or liabilities) extending many decades into the future, obtaining a market-consistent calibration would require quoted prices for options with a similar maturity. Such options are very illiquid and this leads to complications in attempting to obtain risk-neutral valuations.

Third, one of the novelty of our pricing framework draws from the empirical observation that CDS spreads are non-stationary and they are governed by a regime switching dynamics, as assessed by the Bai and Perron test. Experts also agree that countries like Greece defaults every thirty-forty years, so it would be very unrealistic to assume a CDS dynamics floating around a long-term average. To the best of our knowledge, we do not know of any tractable (or theoretical) risk-neutral model to address such an issue.

4.2. *State contingent pricing and holding period returns*

For risk management we need the price (equivalently, return) probability distribution of financial instruments at the risk horizon to compute risk measures or for portfolio optimization or credit value adjustments. Such distributions are conditioned on the relevant risk factors and are needed under the true, objective, probability measure. See Mulvey & Zenios (1994) for generation and use of these distributions for fixed income securities and Consiglio & Zenios (2016) for use in risk management for sovereign debt restructuring.

Given the stochastic dynamics of a risk factor, a closed form expression of the expected value of the pricing function is not always available, especially when there are more than one risk factors. Hence, we resort to the numerical *Least Square Montecarlo* — LSM in short — of Longstaff & Schwartz (2001). This method was developed to price American options and can be suitably modified to compute the conditional expectation of the S-CoCo bond contingent on the short rate r_t and the trigger binary function $\mathbb{1}_\Lambda(t)$.

LSM is based on backward induction whereby the expected value of the (discounted) asset payoff at $t+1$ is approximated by a function of the realizations of the random variable at t:

$$E[V_{t+1}(X_{t+1}) \,|\, X_t = x_t] \approx f_t(x_t, \beta_t), \quad x_t \in \mathbb{R}^d. \qquad (4.6)$$

In the S-CoCo context, $X_t = (r_t, \mathbb{1}_\Lambda)$ is the 2-dimensional vector which takes values $x_t = (r_t^l, \mathbb{1}_{\Lambda^l})$ obtained by the Montecarlo pricing simulation.

The payoff function $V_{t+1}(X_{t+1})$ has to account for the cashflow occurring at $t+1$. This is made up by the possible coupon payment, plus the expected value of the S-CoCo at $t+1$. For a given realization of the random variable X_{t+1}, we have

$$V_{t+1}(r_{t+1}^l, \mathbb{1}_{\Lambda^l}(t+1)) = [\mathbb{P}_{t+1}(r_{t+1}^l, \mathbb{1}_{\Lambda^l}(t+1)) + c\mathbb{1}_{\Lambda^l}(t+1)]B^l(t, t+1), \quad (4.7)$$

where $\mathbb{P}_{t+1}(r_{t+1}^l, \mathbb{1}_{\Lambda^l}(t+1))$ is the regression function approximating the expected S-CoCo price in the next period and $B^l(t, t+1)$ is the discount factor.

Starting from $V_T(x)$ (see discussion below about the terminal payoff function), we estimate backwards the parameters $\beta_t \in \mathbb{R}^M$ and the error term $\epsilon_t \in \mathbb{R}$ that best first the expected value

$$\mathbb{P}_t(x_t, \beta_t) + \epsilon_t = E[V_{t+1}(X_{t+1}) \mid X_t = x_t], \quad (4.8)$$

where $\mathbb{P}_j(\cdot)$ is obtained as a linear combination of basis functions

$$\mathbb{P}_t(x_t, \beta_t) = \sum_{k=1}^{M} \beta_{tk} \phi_k(x_t). \quad (4.9)$$

The choice and the number of basis functions ϕ_k depend on the characteristics of the problem under review. Most authors suggest a trial-and-error approach, starting from simple basis functions and then increase their complexity (for example, using power function with dampening factors, Hermite or Laguerre polynomials), together with statistical selection procedures to find the optimal number of functions. Following (Glasserman 2003, p. 462) we set $\phi_k(r_t) = r_t^k$ and $\phi_k(\mathbb{1}_\Lambda(j)) = \mathbb{1}_\Lambda(t)$. For the short rate we tried different sets of basis functions $\{r_t^k\}_0^{M-1}$, where $M = 3, 4, 5$. For the binary variable, we only considered $k = 1$ since any power of $\mathbb{1}_\Lambda(t)$ will deliver the same value.

Given the sample values for r_t^l, $\mathbb{1}_{\Lambda^l}(t)$ and V_{t+1}^l, starting from $j = T$ and proceeding backwards until $t = 1$, we estimate $\{\beta_{tk}\}_{k=0}^{M}$ through standard OLS. The price of the S-CoCo at $t = 0$ is given by

$$P_0^{\text{LSM}} = \frac{1}{N} \sum_{l \in \Omega} \{[\mathbb{P}_1(r_1^l, \mathbb{1}_{\Lambda^l}(1)) + c\mathbb{1}_{\Lambda^l}(1)]B(0, 1)\}. \quad (4.10)$$

As discussed in Sec. 4.1, the standstill provision allows for principal payment to be postponed if the triggering event occurs within K periods before maturity. Therefore, at $j = T$ the value of the S-CoCo is contingent on the scenario l and is given by

$$V_T^l(x_T^l) = \begin{cases} \mathbb{B}(T, T + \Delta T^l), & \text{if } T \in \Lambda^l, \\ 1 + c, & \text{if } T \notin \Lambda^l, \end{cases} \quad (4.11)$$

where $\mathbb{B}(T, T + \Delta T^l)$ is the expected value of a zero coupon bond maturing at $T + \Delta T^l$. To compute $\mathbb{B}(T, T + \Delta T^l)$, we apply again LSM with r_t^l the only conditioning variable, for $t = T, T+1, \ldots, T + \Delta T^l$, and terminal value $V_{T+\Delta T^l} = 1$.

Table 3 compares the results obtained using different sets of basis functions $\{r_t^k\}_0^{M-1}$ and the dummy variable $\mathbb{1}_\Lambda(j)$. The prices $\bar{P}_0^{\text{LSM}}$ in Table 3 are average

Table 3. Average LSM price at the root node and mean absolute percentage error (MAPE) with respect to Montecarlo pricing for different basis function sets.

| Basis functions	$\bar{P}_0^{\text{LSM}}$	MAPE
$1, r, \mathbb{1}_\Lambda$	0.95558736	0.09163%
$1, r, r^2, \mathbb{1}_\Lambda$	0.96610208	0.08913%
$1, r, r^2, r^3, \mathbb{1}_\Lambda$	0.95644892	0.33191%
$1, r, r^2, r^3, r^4, \mathbb{1}_\Lambda$	0.97058076	1.67800%

prices of an S-CoCo with ten year maturity,[e] obtained by changing the seed of the random engine to generate 5000 sample paths of length ten years of short rates and CDS spreads, keeping the regimes from Sec. 4.1. In the same table we show the mean absolute percentage error with respect to the Montecarlo price. (For a true comparison we need a price obtained through a completely different approach, which, at the moment, is not available for S-CoCo.) The experiment highlights that basis functions up to degree two deliver satisfactory approximations.

However, the objective is not to provide an alternative pricing method, but to determine the future distribution of prices for risk management. We apply LSM to price a 20 year S-CoCo for Greece, Italy, and Germany, and obtain price distributions at 1, 5, 13 and 19.5 years. CDS spread and short rate dynamics are calibrated on the same set of data as in Sec. 4.1. Experiments are carried out for 100 regime scenarios, and 1000 CDS spread scenarios for each regime scenario. Box-Whiskers plots illustrate in Fig. 10 the distributions for $\bar{s} = 200$, where a red star indicates the average and a black dot the median of the price distributions. Price distributions converge to an expected price of par at maturity and this pull-to-par phenomenon shrinks the variability of price distributions near maturity. The distributions are skewed and bimodal (bi-modality is not seen from the Box-Whiskers plot but is evident when plotting the histogram). These results are intuitive and the contribution of our paper is to quantify them. These price distributions can be used to compute holding period returns at different horizons for risk management (Mulvey & Zenios 1994). In Consiglio & Zenios (2015) we use holding period return distributions to illustrate how S-CoCo could improve the risk profile of a eurozone crisis country.

4.3. *The effect of regime switching on state contingent prices*

To gain further insights in the performance of S-CoCo, we numerically test the effects of regime switching. Italy is used in all experiments, with thresholds 200 and 500. In the former case the standstill is activated and the results are qualitatively similar to what one would expect for Greece as well. In the latter case the standstill is very rarely triggered and the results are very different from those of Greece.

---

[e]A shorter maturity is used to reduce computational time, but similar results are obtained when running the experiment for a 20 year bond on a single set of basis functions.
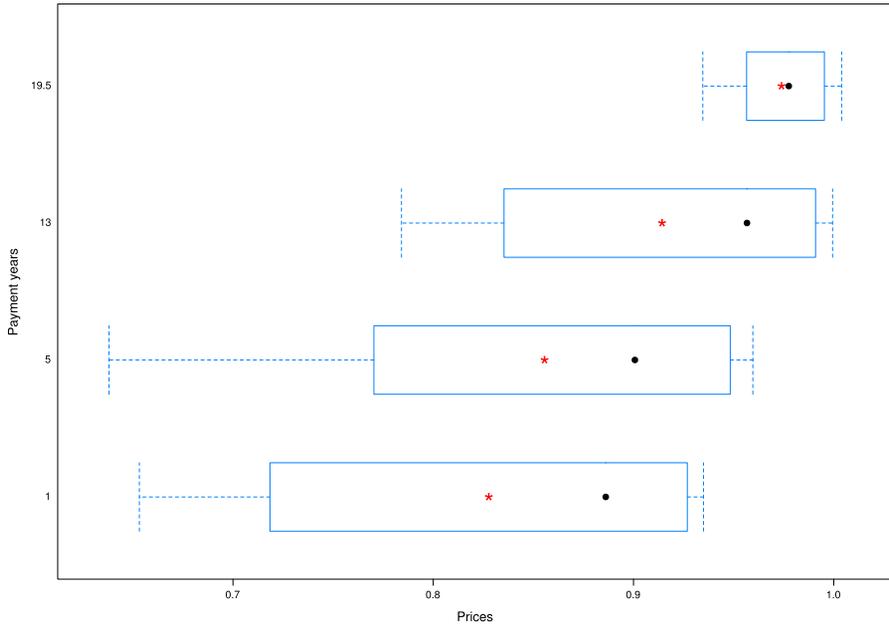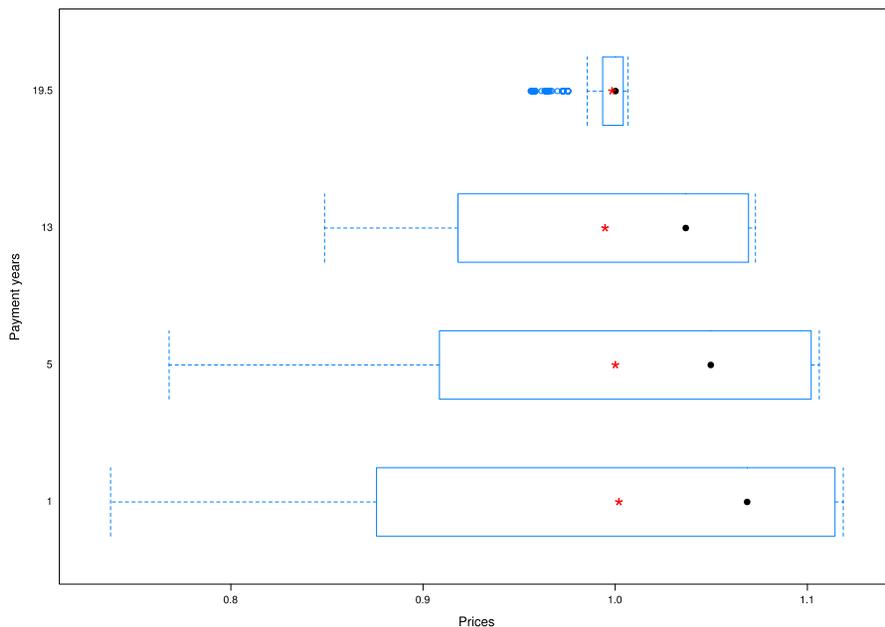
(a) Greece
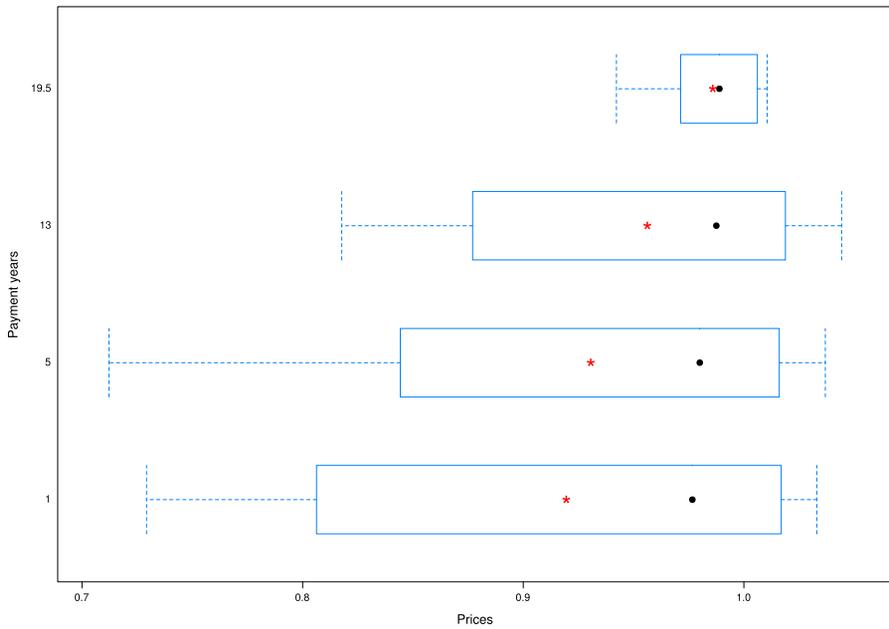
(b) Italy

Fig. 10. Price distribution of 20 year S-CoCo with threshold 200 at 1, 5, 13, and 19.5 years. Price distributions converge to an expected price of par at maturity and this pull-to-par phenomenon shrinks the variability of price distributions near maturity.

(c) Germany

Fig. 10. (*Continued*)

Results are reported again for a 20 year S-CoCo price distribution at 1, 5, 13, and 19.5 years, but under different scenario test beds with and without regime switching. In particular:

R-OFF No regime switching, with the parameters used to calibrate the CDS spread model set to their historical average and simulating 5000 CDS spread and interest rate scenarios.

R-1 Only one scenario of regime switching between the identified regimes with 5000 CDS spread and interest rate scenarios.

R-100 100 simulations of regime switching between the identified regimes and 1000 scenarios of CDS spread and interest rates for each regime scenario.

Figures 11–13 show the distribution of the prices for the three scenario test beds. The following observations can be made:

(1) With the regime scenario simulation switched off and the CDS spread calibrated to the historical average, the S-CoCo with threshold 200 exhibits an (almost) binary distribution, while at threshold 500 its prices are just like a straight bond. Under the historical average regime the Italian CDS spreads do not exhibit sufficient variability to trigger the S-CoCo. Payment standstill becomes an extremely rare event, but with big impact.
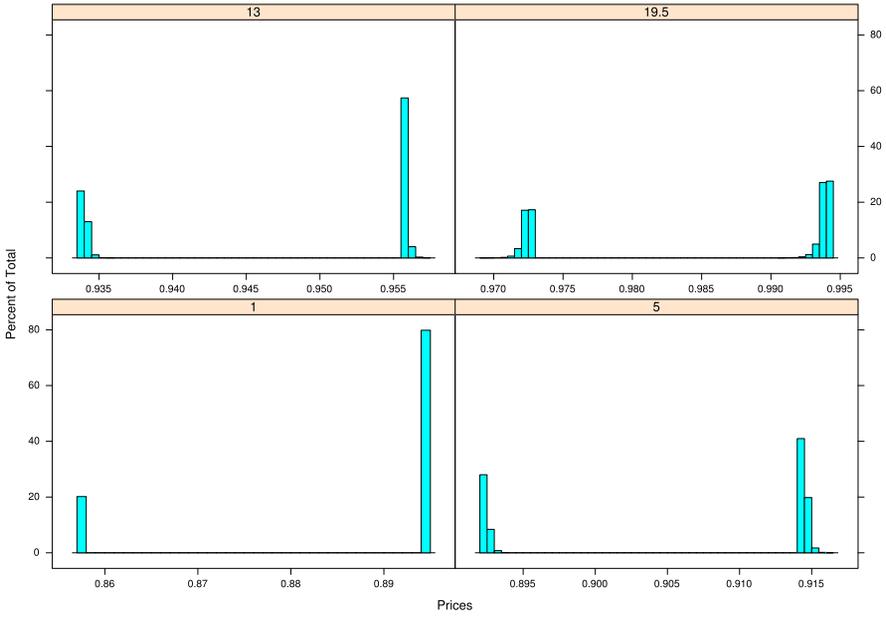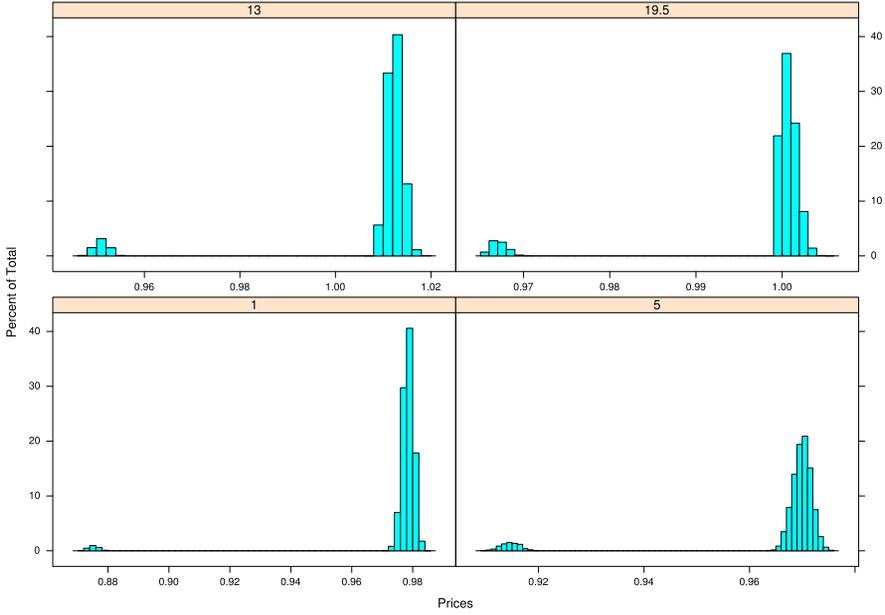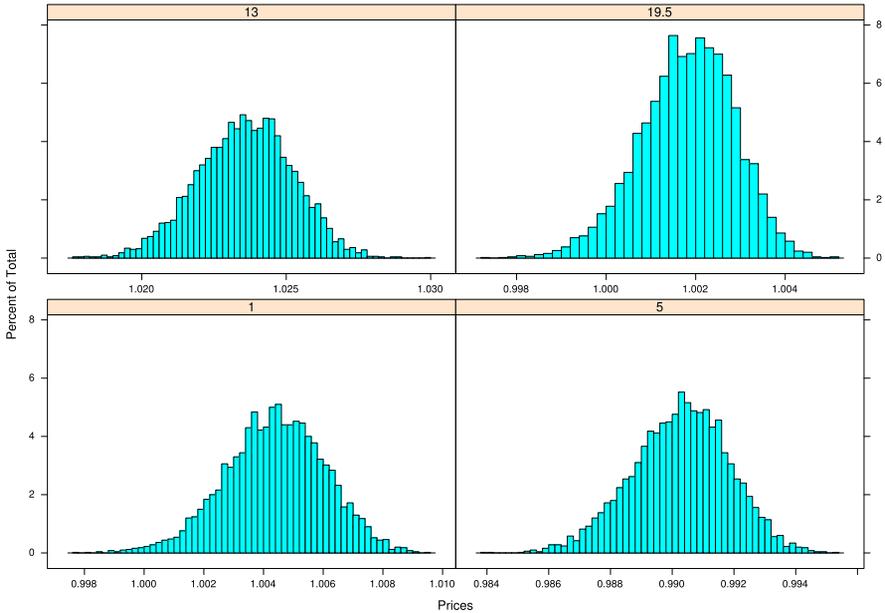
(a) Threshold 200
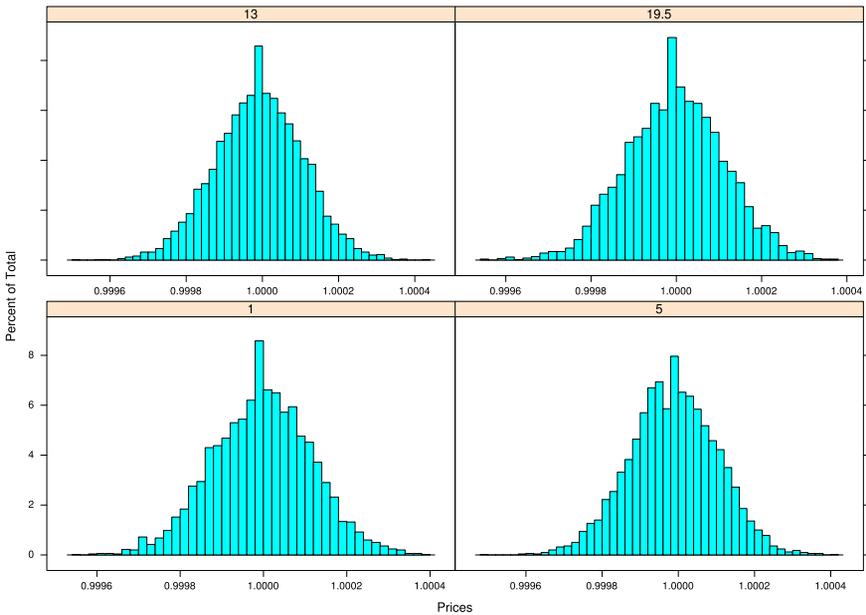
(b) Threshold 500

Fig. 11. Price distribution of twenty-year Italian S-CoCo at different risk horizons without regime switching (test bed `R-OFF`). S-CoCo with low threshold (top) exhibits an (almost) binary distribution because most of the scenarios trespasses the threshold so they price below the par. For high value of the threshold (bottom) its prices are just like a straight bond.
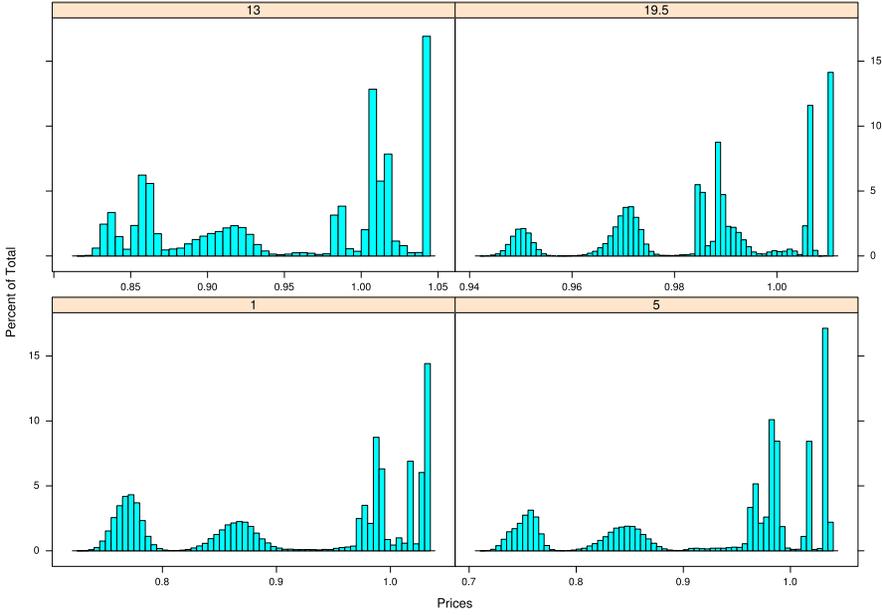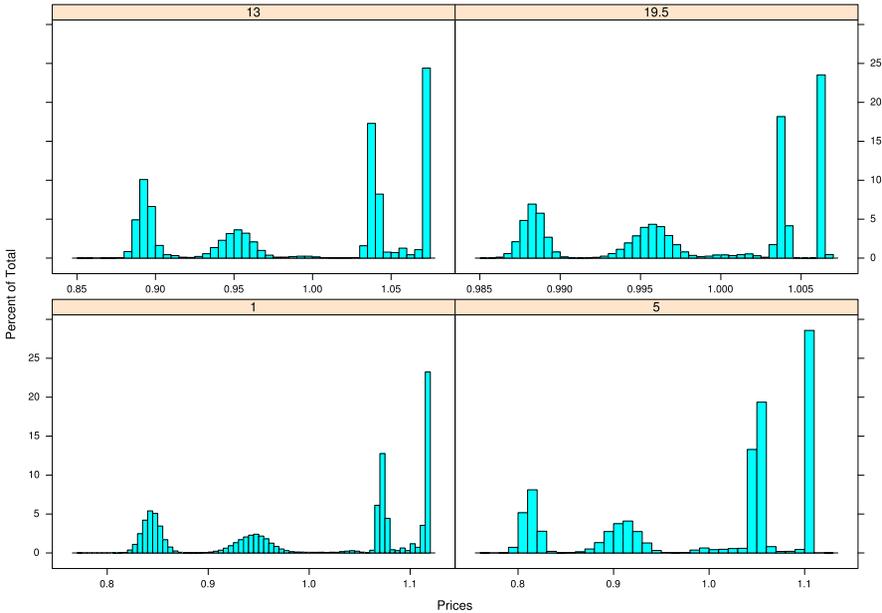
Fig. 12. Price distribution of twenty-year Italian S-CoCo at different risk horizons with only one regime switching scenario (test bed R-1). (a) In this case, regimes switch from tranquil levels into turbulence and even a crisis, and for a low threshold and (b) the price distribution exhibits more variability, while a nontrivial effect is found for a high threshold.

(a) Threshold 200

(b) Threshold 500

Fig. 13. Price distribution of twenty-year Italian S-CoCo at different risk horizons with multiple regime switching scenarios (test bed `R-100`). When both regime switching and CDS spreads are simulated properly, S-CoCos price exhibits a multi-modal distributions at the risk horizon, as a result of a combination of regime switching and standstill triggers.

(2) When introducing even one regime scenario, capturing the observation of the recent past that Italy may move from a tranquil regime into turbulence and even a crisis, then the distribution of prices at threshold 200 exhibits more variability. There is also a non-trivial effect for threshold 500, although significantly lower than at the 200 threshold.

(3) Finally, when simulating properly both regime switching and CDS spreads we obtain multi-modal distributions at the risk horizon. These modalities result from a combination of regime switching and standstill triggers.

The multi-modality of the distributions, when simulated properly, may be disconcerting. This is inescapable when modeling events with large impact — such as regime switching — and limited historical data to calibrate. If we could offer a criticism to our modeling approach is that a regime derived from expert opinion — such as "after the Brexit referendum, Italian CDS spreads will reach levels seen at the peak of the Eurozone crisis and stay there until the Brexit issue is resolved" — maybe more appropriate than a statistical model. If an expert opinion regime is available, the pricing model applies with `R-OFF`.

4.4. *Dual trigger pricing*

McDonald (2013) argues that bank CoCo should not be converted for idiosyncratic problems but only when the entity's difficulties come with market-wide problems. He illustrates dual trigger structures with a simple pricing example. The arguments for dual triggers seem well accepted for corporate debt where firms should be allowed to fail when they face difficulties in a benign market, but not when they face problems during a market-wide crisis. Sovereigns, on the other hand, do not fail, and Consiglio & Zenios (2015) "do not see any arguments in favor of a dual trigger, although an additional market-specific indicator could be introduced to allow for potential [sovereign] default". However the debate on sovereign contingent debt is at an early stage, and should dual price trigger be considered necessary we could use a systemic market index such as the CBOE volatility index VIX, or the emerging markets EMBI index, or, for eurozone countries, the CDS spreads on AAA-rated sovereigns. If a sovereign's CDS threshold is breached during a systemic crisis as indicated by the market index, then the payment standstill is triggered, but for idiosyncratic crises there would be a different treatment.

We develop here the S-CoCo pricing model with a dual trigger. The model of Sec. 4.1 is extended by augmenting the stochastic process ξ with the market index $v_t, \xi = \{r_t, s_t, v_t\}$. (We assume that the stochastic components of ξ are uncorrelated. More complex patterns of correlation between the market index v_t and r_t and s_t can be introduced, but they are beyond the scope of the present paper.) A trigger threshold $\bar{v}$ relates to the market index v_t, and $\mathcal{T}_m^l$, $m = 1, 2, \ldots, M$, denotes those time sets in which, conditioned on scenario l, there is a coupon payment standstill for K_1 periods.

For the standstill to be triggered both s_t^l and v_t^l must breach their respective thresholds $\bar{s}$ and $\bar{v}$ at time t. But we also need to model situations, where the market and the country specific indices decouple, to account for idiosyncratic crises. There are different patterns of aid that can be envisioned for such eventualities, which are represented using a different standstill period, K_2. We embrace the view that countries in financial distress for purely idiosyncratic reasons need more help and therefore $K_2 > K_1$.

If at time t, and under scenario l, the CDS rate s_t^l hits $\bar{s}$, and the market index v_t^l is below $\bar{v}$, coupon payments are suspended for K_2 periods. Denote by $\mathcal{V}_q^l = \{t, t+1, \ldots, t+K_2\}$, $q = 1, 2, \ldots, Q$, such time sets with the same properties as $\mathcal{T}_m^l$. The time sets defining the dual trigger mechanism are then given by

$$\Lambda^l = \bigcup_{m=1}^{M} \mathcal{T}_m^l, \quad \Upsilon^l = \bigcup_{q=1}^{Q} \mathcal{V}_q^l, \tag{4.12}$$

and the new indicator function $\mathbb{1}_{\Upsilon^l} : \mathcal{T} \to \{0, 1\}$ is

$$\mathbb{1}_{\Upsilon^l}(t) = \begin{cases} 0, & \text{if } t \in \Upsilon^l, \\ 1, & \text{if } t \notin \Upsilon^l. \end{cases} \tag{4.13}$$

The S-CoCo price function (4.3) with a dual trigger becomes

$$P_0 = \frac{1}{N} \sum_{l \in \Omega} \sum_{t \in \mathcal{T}} B^l(0, t) \left(\mathbb{1}_{\Lambda^l}(t) \cdot \mathbb{1}_{\Upsilon^l}(t) \right) c + B^l(0, T + \Delta T^l). \tag{4.14}$$

Note that, since $\mathcal{T}_m^l \cap \mathcal{V}_q^l = \emptyset$, for any $m = 1, 2, \ldots, M$, and $q = 1, 2, \ldots, Q$, then also $\Lambda^l \cap \Upsilon^l = \emptyset$, and the product of the two indicator functions correctly represents the dual trigger mechanism.

5. Conclusions

We have developed a pricing model for sovereign contingent convertible bonds with payment standstill that captures the regime-switching nature of the triggering process. We have adapted an existing single-factor tractable stochastic model of spread-returns with mean-reversion to model spread levels converging to a long-term steady state value estimated from market data, whereby the steady state is modeled by a novel regime switching Markov process model. The Monte Carlo simulation pricing model is embedded in the Longstaff–Schwartz framework to compute state contingent prices at some risk horizon. This facilitates risk management.

Extensive numerical experiments illustrate the performance of the models and shed light on the performance of sovereign contingent debt. In particular, we observe the skewed distribution of prices at the risk horizon, the pull-to-par phenomenon as securities approach maturity, and the multi-modality of the price distribution as the underlying CDS process switches regimes and/or the payment standstill is triggered.

The models are applied to S-CoCo designs for Greece, Italy, and Germany, in order to illustrate how these instruments would be priced for countries under different economic conditions. The results are intuitive and the contribution of the paper is in providing a model to quantify prices and holding period returns. Such a model is an essential tool if sovereign contingent debt is to receive attention and eventual acceptance as a practical financial innovation response to the problem of debt restructuring in sovereign debt crises. In a companion paper, we showed how these models can be used to develop a sovereign debt risk optimization model to improve a country's risk profile (Consiglio & Zenios 2015).

Acknowledgments

Appendix A. Asymptotic Modeling of the Scenario Generating Process

We determine the parameters of the model for CDS spread return to identify its asymptotic dynamics. We start from the discrete time model of (O'Donoghue *et al.* 2014, cf. Eq. (2), or Eq. (6) without the jump term) and derive a set of conditions on the asymptotic moments to be matched with empirically estimated values. To simplify the notation in their Eqs. (2) or (6), set $k_0 = \gamma$, $k_1 = \alpha + \beta$ and $k_2 = \alpha\beta$, to get

$$\Delta r_t = \left(k_0 - k_1 r_t - k_2 \sum_{s=0}^{t} r_s \Delta t \right) \Delta t + \sigma w_t, \tag{A.1}$$

where r_t is the return at time t and $w_t \sim \mathcal{N}(0, \Delta t)$.

The simulation model is made up of two stochastic equations, one for the CDS and one for the interest rate, identical structure given by (A.1). In case the two factors are correlated, we need two noise components, $\epsilon_t^1, \epsilon_t^2 \sim \mathcal{N}(0, \Delta t)$, with $\rho(\epsilon_t^1, \epsilon_t^2) = 0$. It can be easily shown that the two processes w_t^1 and w_t^2, given by

$$w_t^1 = \epsilon_t^1, \tag{A.2}$$

$$w_t^2 = \rho \epsilon_t^1 + \epsilon_t^2 \sqrt{(1 - \rho^2)}, \tag{A.3}$$

have correlation ρ, to be estimated from available historical time series.

Following O'Donoghue *et al.* (2014), for $t \to \infty$, we have

$$\mathbb{E}[r_t] = 0, \tag{A.4}$$

$$\text{var}[r_t] = \frac{\sigma^2}{2k_1}, \tag{A.5}$$

$$\mathbb{E}[C_t] = \frac{k_0}{k_2}, \tag{A.6}$$

$$\text{var}[C_t] = \frac{\sigma^2}{2k_1 k_2}, \tag{A.7}$$

where $C_t = \sum_{s=0}^{t} r_s \Delta t$ and C_t is normally distributed.

The spread process $S_t = S_0 \exp(C_t)$ is log-normally distributed with

$$\mathbb{E}[S_t] = S_0 \exp\left(\frac{k_0}{k_2} + \frac{\sigma^2}{4k_1 k_2}\right), \tag{A.8}$$

$$\text{var}[S_t] = S_0^2 \exp\left(2\frac{k_0}{k_2} + \frac{\sigma^2}{2k_1 k_2}\right)\left[\exp\left(\frac{\sigma^2}{2k_1 k_2}\right) - 1\right]. \tag{A.9}$$

We now have three equations in the four unknowns of the stochastic dynamics (A.1). We need one additional condition which we derive from the squared changes $\mathbb{E}[(\Delta r_t)^2]$, which is a measure of the smoothness of the process. With some standard assumptions for stochastic processes, namely that $\mathbb{E}[w_t C_t] = 0$, $\mathbb{E}[r_t C_t] = 0$ and $\mathbb{E}[r_t w_t] = 0$, and using simple algebra, we obtain

$$\mathbb{E}[(\Delta r_t)^2] = \frac{\sigma^2}{2}\left(k_1 + \frac{k_2}{k_1} + 2\right). \tag{A.10}$$

A sample estimate $\hat{s}^2$ for $\mathbb{E}[(\Delta r_t)^2]$ is given by

$$\hat{s}^2 = \frac{1}{N}\sum_{t=1}^{N}(r_t - r_{t-1})^2. \tag{A.11}$$

The theoretical moments defined by (A.5), (A.8), (A.9), and of the smoothness (A.10) are then matched to the empirical observations. We denote by $\hat{S}$ the asymptotic CDS spread level, by $\hat{\sigma}_S$ the asymptotic variance of CDS spread level, by $\hat{\sigma}_r$ the asymptotic variance of CDS spread returns, and by $\hat{s}^2$ the smoothness of the CDS spread level. (These quantities are estimated for each regime separately if regime switching is manifested in the empirical data, e.g. Table 2.) Denoting by T_τ the set of time periods in regime τ, we obtain the following moment estimates for the regime:

$$\hat{S} = \frac{1}{|T_\tau|}\sum_{t \in T_\tau} S_t, \tag{A.12}$$

$$\hat{\sigma}_S^2 = \frac{1}{|T_\tau|}\sum_{t \in T_\tau}(S_t - \hat{S})^2, \tag{A.13}$$

$$\hat{\sigma}_r^2 = \frac{1}{|T_\tau|}\sum_{t \in T_\tau}(r_t - \hat{r})^2. \tag{A.14}$$

Similarly, we have the estimate of the smoothness of the regime:

$$\hat{s}^2 = \frac{1}{|T_\tau|} \sum_{t \in T_\tau} (r_t - r_{t-1})^2. \tag{A.15}$$

If S_0 denotes the starting value of the CDS spread for the selected regime, we can match the theoretical moments to their estimated values solving the system of nonlinear equations in k_0, k_1, k_2, and σ:

$$\exp\left(\frac{k_0}{k_2} + \frac{\sigma^2}{4k_1 k_2}\right) = \frac{\hat{S}}{S_0}, \tag{A.16}$$

$$\exp\left(2\frac{k_0}{k_2} + \frac{\sigma^2}{2k_1 k_2}\right)\left[\exp\left(\frac{\sigma^2}{2k_1 k_2}\right) - 1\right] = \frac{\hat{\sigma}_S^2}{S_0^2}, \tag{A.17}$$

$$\frac{\sigma^2}{2k_1} = \hat{\sigma}_r^2, \tag{A.18}$$

$$\frac{\sigma^2}{2}\left(k_1 + \frac{k_2}{k_1} + 2\right) = \hat{s}^2. \tag{A.19}$$

(Of course the right hand side parameters do not have to be estimated from historical data, but can be values assumed or estimated by the user. For instance, the
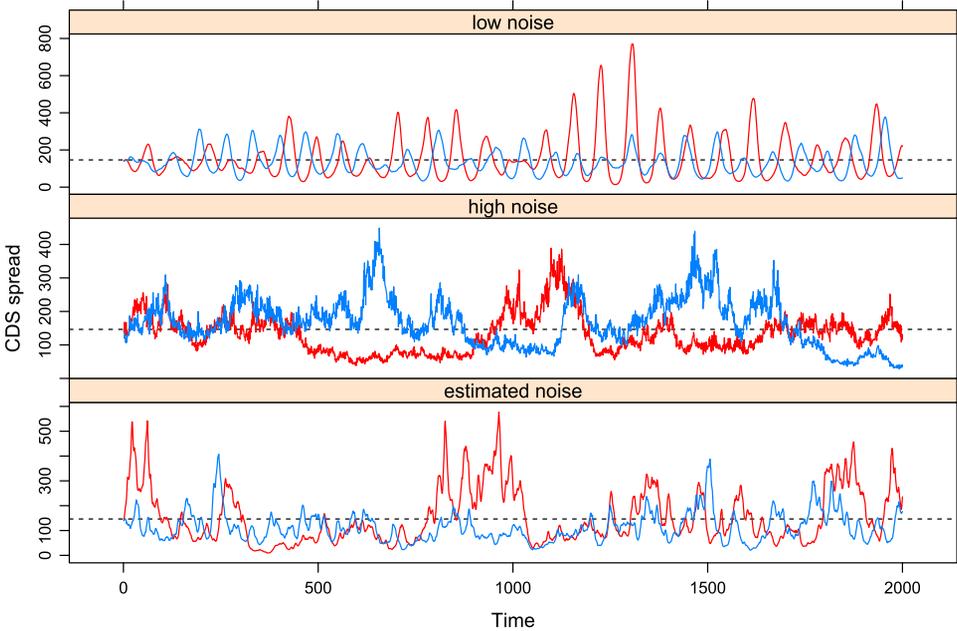

Fig. A.1. The effect of the parameter σ on the smoothness of CDS spread dynamics. In the upper panel we use a low value of the parameter σ, in the middle panel we use a high value of σ, and in the bottom panel we use σ estimated from Eq. (A.11). The dotted lines show the asymptotic level of the CDS spread.

user may wish to price the instruments for extreme values of the moments, or the values implied by the rating of a country.)

The closed form solution to the system of Eqs. (A.16)–(A.19) is given by

$$k_0 = \frac{\hat{\sigma}_r^2}{\log\left(1 + \frac{\hat{\sigma}_S^2}{\hat{S}^2}\right)} \log\left(\frac{\hat{S}}{S_0}\right) - \frac{1}{2}\hat{\sigma}_r^2, \tag{A.20}$$

$$k_1 = \frac{\sigma^2}{2\hat{\sigma}_r^2}, \tag{A.21}$$

$$k_2 = \frac{\hat{\sigma}_r^2}{\log\left(1 + \frac{\hat{\sigma}_S^2}{\hat{S}^2}\right)}, \tag{A.22}$$

$$\sigma^2 = 2\hat{\sigma}_r^2 \left[-1 + \sqrt{1 + \frac{\hat{s}^2 - k_2\hat{\sigma}_r^2}{4\hat{\sigma}_r^2}}\right]. \tag{A.23}$$

Finally, to ensure that $\sigma \in \mathbb{R}^+$ we need $\hat{s}^2 - k_2\hat{\sigma}_r^2 > 0$.

We point out the role of the noise term σ on the smoothness of the process. Figure A.1 illustrates the effect of σ on two paths generated obtained from (A.1). Observe that the lower the σ, the smoother is the generated curve, so σ relates to $\mathbb{E}[(\Delta r_t)^2]$. In the same figure we illustrate the two paths when calibrated on a value estimated from historical data using the system of equations above.

References

C. Alexander & A. Kaeck (2008) Regime dependent determinants of credit default swap spreads, *Journal of Banking and Finance* **32** (6), 1008–1021.

J. Amato & E. Remolona (2003) The credit spread puzzle, *BIS Quarterly Review* 51–63.

M. G. Arghyrou & A. Kontonikas (2016) The EMU sovereign-debt crisis: Fundamentals, expectations and contagion, *Journal of International Financial Markets, Institutions and Money* **22** (4), 658–677.

P. Augustin (2014) Sovereign credit default swap premia, *Journal of Investment Management* **12** (2), 65–102.

S. Badaoui, L. Cathcart & L. El-Jahel (2013) Do sovereign credit default swaps represent a clean measure of sovereign default risk? A factor model approach, *Journal of Banking & Finance* **37** (7), 2392–2407.

J. Bai & P. Perron (1998) Evaluating and testing linear models with multiple structural changes, *Econometrica* **66** (1), 47–78.

Bank of England (2015) Workshop summary. In *Bank of England Workshop on GDP Linked Bonds*. Bank of England, http://www.bankofengland.co.uk/research/Pages/conferences/301115.aspx.

B. Barkbu, B. Eichengreen & A. Mody (2012) Financial crises and the multilateral response: What the historical record shows, *Journal of International Economics* **88** (2), 422–435.

E. Borensztein & P. Mauro (2004) The case for GDP-indexed bonds, *Economic Policy* **19** (38), 165–216.

D. Brigo & A. Alfonsi (2005) Credit default swaps calibration and option pricing with the SSRD stochastic intensity and interest-rate model, *Finance and Stochastics* **9** (1), 29–42.

M. Brooke, R. Mendes, A. Pienkowski & E. Santor (2013) Sovereign default and state-contingent debt. Financial Stability Paper No. 27, Bank of England.

C. Calomiris & R. J. Herring (2013) How to design a contingent convertible debt requirement that helps solve our too-big-to-fail problem, *Journal of Applied Corporate Finance* **25**, 21–44.

R. Castellano & L. Scaccia (2014) Can CDS indexes signal future turmoils in the stock market? A Markov switching perspective, *Central European Journal of Operations Research* **22** (2), 285–305.

Y. Censor & S. A. Zenios (1997) *Parallel Optimization*: *Theory*, *Algorithms*, *and Applications*. New York: Oxford University Press.

A. Consiglio & S. A. Zenios (2015) The case for contingent convertible debt for sovereigns. Working Paper 15-13, The Wharton Financial Institutions Center, University of Pennsylvania, Philadelphia. Available at http://papers.ssrn.com/sol3/papers.cfm?abstract_id=2478380.

A. Consiglio & S. A. Zenios (2016) Risk management optimization for sovereign debt restructuring, *Journal of Globalization and Development* **6** (2), 181–214.

A. Consiglio & S. A. Zenios (2018) Pricing and hedging GDP-linked bonds in incomplete markets, *Journal of Economic Dynamics and Control* **88**, 137–155.

A. Consiglio, S. Lotfi & S. A. Zenios (2017) Portfolio diversification in the sovereign CDS market, *Annals of Operations Research* **266** (1–2), 5–33.

R. Cont & Y.-H. Kan (2011) Statistical modeling of credit default swap portfolios. Available at SSRN: http://ssrn.com/abstract=1771862.

A. Drud (2005) CONOPT. In *GAMS*: *The Solvers Manual*. GAMS Development Corporation.

F. Fabozzi, R. Giacometti & N. Tsuchida (2016) Factor decomposition of the eurozone sovereign CDS spreads, *Journal of International Money and Finance* **65**, 1–23.

A. Fontana & M. Scheider (2010) An analysis of euro area sovereign CDS and their relation with government bonds. Working Paper 1271, European Central Bank.

P. Glasserman (2003) *Monte Carlo Methods in Financial Engineering*. New York: Springer-Verlag.

F. F. Heinz & Y. Sun (2014) Sovereign CDS spreads in Europe — The role of global risk aversion, economic fundamentals, liquidity and spillovers. Working paper WP/14/17, International Monetary Fund, Washington, DC.

IMF (2017a) State-contingent debt instruments for sovereigns. Staff report, International Monetary Fund.

IMF (2017b) State-contingent debt instruments for sovereigns–annexes. Staff report, International Monetary Fund.

M. Kamstra & R. J. Shiller (2009) The case for trills: Giving the people and their pension funds a stake in the wealth of the nation, Discussion Paper 1717, Cowles Foundation for Research in Economics, Yale University, New Haven, CT.

J. N. Kapur (1989) *Maximum-Entropy Models in Science and Engineering*. India: Wiley.

S. Kotz, N. Balakrishnan & N. L. Johnson (2005) Dirichlet and inverted Dirichlet distributions. In: *Continuous Multivariate Distributions*, chapter 49, pp. 485–527. John Wiley & Sons, New York.

Y. Li (2016) The long march towards an international legal framework for sovereign debt restructuring, *Journal of Globalization and Development* **6** (2), 329–341.

F. A. Longstaff & E. S. Schwartz (2001) Valuing American options by simulation: A simple least-squares approach, *The Review of Financial Studies* **14** (1), 113–147.

F. A. Longstaff, J. Pan, L. H. Pedersen & K. J. Singleton (2011) How sovereign is sovereign credit risk? *American Economic Journal: Macroeconomics* **3**, 75–103.

R. L. McDonald (2013) Contingent capital with a dual price trigger, *Journal of Financial Stability* **9** (2), 230–241.

J. M. Mulvey & S. A. Zenios (1994) Capturing the correlations of fixed-income instruments, *Management Science* **40**, 1329–1342.

B. O'Donoghue, M. Peacock, J. Lee & L. Capriotti (2014) A spread-return mean-reverting model for credit spread dynamics, *International Journal of Theoretical and Applied Finance* **17** (3), 1450017.

M. H Schneider & S. A. Zenios (1990) A comparative study of algorithms for matrix balancing, *Operations Research* **38** (3), 439–455.

C. E. Shannon (1948) A mathematical theory of communication, *The Bell System Technical Journal* **27** (3), 379–423.